U–Pb LA–ICP–MS dating of zoned zircons from the Greater Caucasus pre-Alpine crystalline basement: Evidence for Cadomian to Late Variscan evolution

IRAKLI GAMKRELIDZE[1,✉], DAVID SHENGELIA[1], GIORGI CHICHINADZE[1], YUAN-HSI LEE[2], AVTANDIL OKROSTSVARIDZE[3], GIORGI BERIDZE[1] and KRISTINA VARDANASHVILI[1]

[1]A. Janelidze Institute of Geology of I. Javakhishvili Tbilisi State University, Politkovskaia 31, 0185, Tbilisi, Georgia;
✉gamkrelidze77@gmail.com
[2]National Chung-Cheng University, Daxue road 168, 62102, Chiayi, Taiwan
[3]Ilia State University, Cholokashvili 3, 0162, Tbilisi, Georgia

Abstract: Here we report U–Pb zircon age data, obtained using LA–ICP–MS, from a total of 14 rocks of the Pass and Elbrus sub-zones of the Main Range Zone of the Greater Caucasus, which differ quite significantly from each other in composition of sedimentary and igneous rocks. Both exotic (detrital) zircons, and those formed within the Greater Caucasus are revealed. The ages of detrital zircons range from 2981 to 668 Ma. On the basis of weighted mean age data among in situ zircons from meta-sedimentary rocks in both sub-zones figures of 626± 2 Ma and 627± 19 Ma were detected, which corresponds to the earliest – Cadomian stage of high temperature regional metamorphism. From meta-sedimentary rocks of the Elbrus sub-zone figures – 461±5.3 Ma, 457±12 Ma indicate manifestation of the Ordovician (tectonically associated with Caledonian orogeny) stage of high temperature prograde regional metamorphism. Figures from granitoid rocks of both sub-zones – 454±9 Ma, 468±5 Ma and 471.7±4.6 Ma were obtained, which also correspond to the Caledonian stage of synmetamorphic granitoid formation. Besides, figures from the meta-sedimentary rocks of the Pass sub-zone – 312.5±4 Ma, 317.0±8.3 Ma correspond to Late Variscan regressive regional metamorphism. In addition, figures obtained from the granitoid rocks of both sub-zones – 309±8 Ma, 310.9 Ma, 325±4 Ma, 311±5.9 Ma and 357±5.9 Ma correspond to the Late Variscan stage of synmetamorphic granitoid formation. These results are in good agreement with geological and petrological data for the Greater Caucasus.

Keywords: Greater Caucasus, crystalline basement, U–Pb dating, regional metamorphism, granitoid magmatism.

Introduction

The Caucasus is a component of the Mediterranean (Alpine–Himalayan) collisional orogenic belt. It presents a complicated polycyclic geological structure involving mountain fold systems of the Greater and Lesser Caucasus and adjacent fore-deeps and intermountain troughs.

Within the oceanic area of Tethys (with a typical oceanic crust), which separated the Afro–Arabian and Eurasian continental plates, in the geological past relatively small continental or subcontinental plates – tectonostratigraphic terranes were situated. They have various geodynamic natures and are characterized by specific lithologic–stratigraphic section and magmatic, metamorphic and structural features.

In the Caucasian segment of the Mediterranean orogenic belt the Greater Caucasian, Black Sea–Central Transcaucasian, Baiburt–Sevanian and Iran–Afghan terranes are identified, representing island arcs or microcontinents in the geological past (Gamkrelidze 1997; Gamkrelidze & Shengelia 2005) (Fig. 1). In terms of modern structure they are accreted terranes of the first order separated by known or assumed ophiolite sutures of different age. Besides, in many places of the Caucasian region there are ophiolite terranes – relics of the oceanic crust of small or large oceanic basins obducted from the above-mentioned ophiolite sutures (Fig. 1).

On the margins of these oceans during the Neoproterozoic and Paleozoic time supra-subduction regional metamorphism and granitoid formation took place.

The age of the Greater Caucasus (GC) crystalline basement constituent rocks is still controversial. For a long time, the age of the source rocks of the basement was considered to be mostly Precambrian, and the regional metamorphism and granitoid formation were pre-Variscan and Variscan (Bessonov 1938; Rubinstein 1970; Baranov & Kropachev 1976; Zaridze & Shengelia 1978; Lebedko & Usik 1985; Grekov & Lavrishchev 2002). However, some authors attribute the process of regional metamorphism only to the Variscan orogeny and the parent rocks, that form the Main Range zone, of the GC (MR GC) are considered to be no older than the Early Paleozoic (Bibikova et al. 1991; Somin et al. 2007; Somin 2011).

In the following studies, most of the authors of the present paper have systematically investigated the pre-Alpine basement of the GC (Shengelia et al. 1991, 1995; Gamkrelidze et al. 1996; Gamkrelidze & Shengelia 2005, 2007; Okrostsvaridze 2007; Okrostsvaridze & Tormay 2011). Several stages
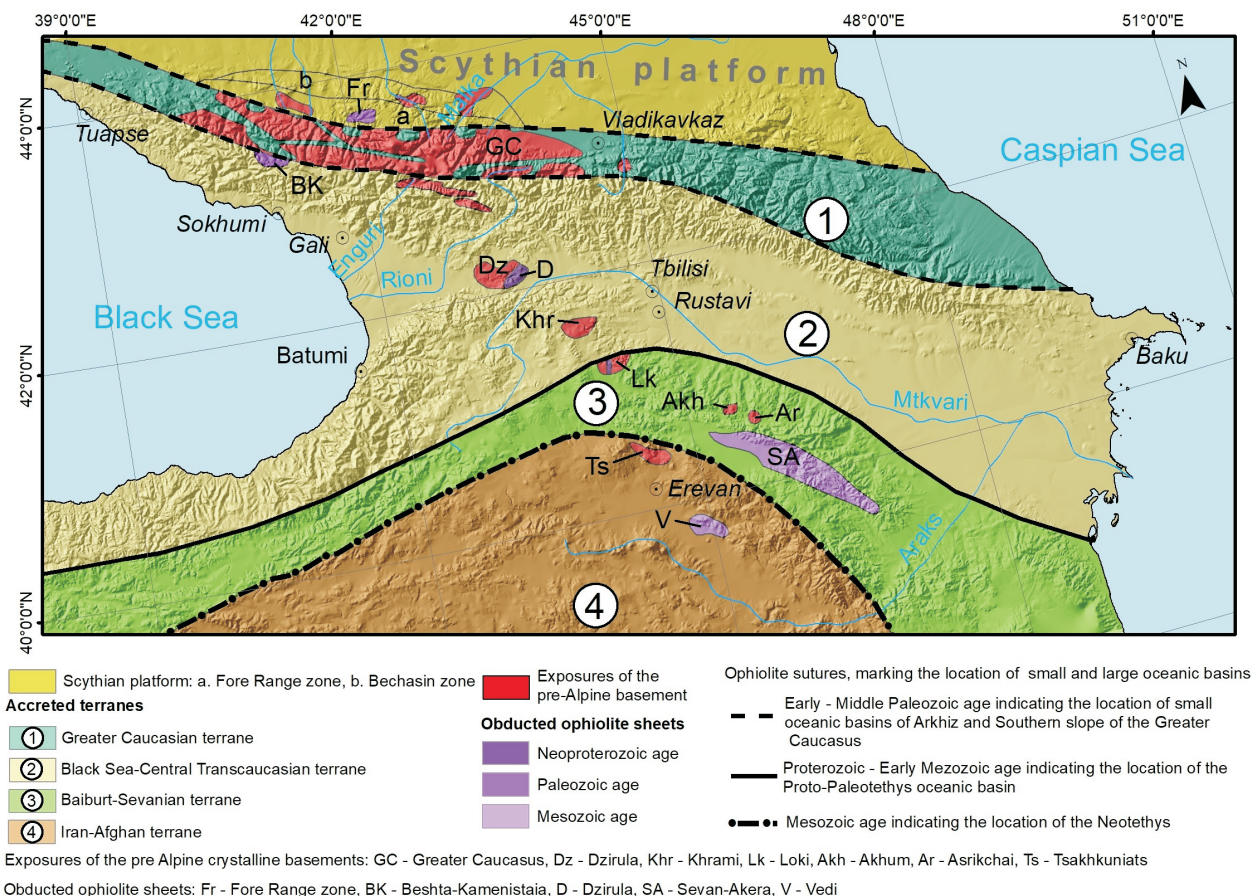
Fig. 1. Tectonic zoning of the Caucasus on the basis of the terrane analysis (Gamkrelidze 1997; Gamkrelidze & Shengelia 2005), simplified.

of pre-Variscan and Variscan regional metamorphism and granite formation have been revealed, based on studies of geological relationships between rock units, and their petrological and geochemical characteristics.

The aim of this work is to fill the gap existing in the geochronological dating of metamorphic and magmatic rocks of the crystalline basement of the GC taking into account quite complete geological and petrological data.

Within the pre-Alpine basement of the GC 3 samples from igneous rocks, 5 samples from meta-igneous rocks and 6 samples from meta-sedimentary rocks of zircons were analysed by U–Pb LA–ICP–MS method.

Geological background and previous geochronological data

At present, the Greater Caucasian terrane corresponds to the Main Range zone of the Greater Caucasus (MR GC) (Fig. 1), which is subdivided into two sub-zones: the Pass sub-zone to the south-west and the Elbrus sub-zone to the north-east (Fig. 2). These two sub-zones differ markedly from each other in terms of their constituent rock composition, character of metamorphism and magmatism and regional structure. In particular, both sub-zones mainly contain metapelites, but

the Pass sub-zone contains abundant metabasites and isolated intrusives mainly of trondhjemites, diorites, gabbro-diorites and granodiorites whereas the Elbrus sub-zone contains rare metabasites but abundant granites. The sub-zones are in tectonic contact with one another along the Alibek–Urukh fault (Fig. 2), which initially formed in pre-Late Paleozoic times, as indicated by the confinement to this fault of apogranitoid blastocataclazites (Somin 1971).

The fault was re-activated in Alpine times because it cuts Jurassic sediments filling a graben-structure confined to it (Fig. 2). Geological observation and character of delineation of the fault plane in relief show that at present, it is a steeply north-dipping, brittle reverse fault with northern upthrow side. But in places, for example, to the north of the upper reaches of the Sakeni and Klichi rivers, the Elbrus sub-zone is overthrust on the Pass sub-zone (Fig. 2).

The Pass sub-zone

The Pass sub-zone consists of the Buulgen and the Laba metamorphic complexes (Fig. 2) but contact relations between them have not been observed. Based on the fact that these complexes rather differ from each other, both in composition and in the degree of metamorphism, we assume that this contact is tectonic and the Buulgen and Laba complexes are of
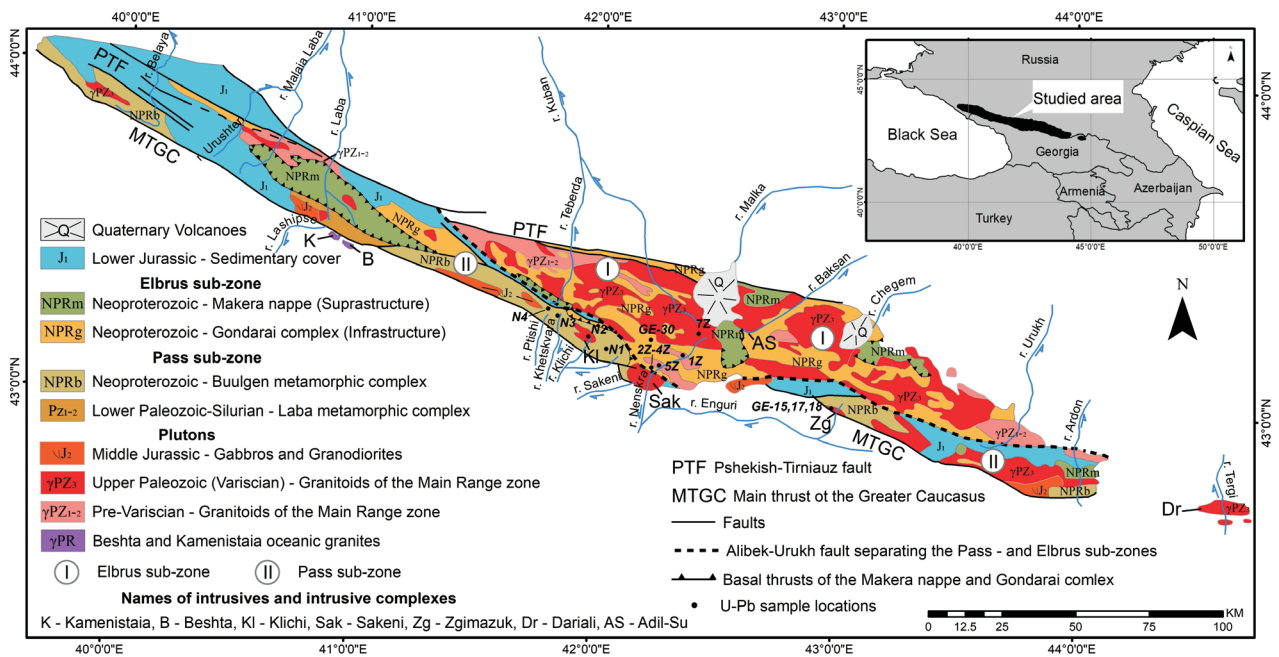
Fig. 2. Scheme of geological structure of the crystalline basement of the Greater Caucasus (Shengelia et al. 1991), modified.

different age. Somin (1991, 2011) argues that some parts of the complexes can be correlated. Adamia (1984), Adamia et al. 2011), and Belov et al. (1978) argue that they are the same age.

The Buulgen metamorphic complex

The complex is subdivided into three suites. In ascending order these are: the Gvandra, Klichi and Sissina suites, which conformably follow one another. They are metamorphosed in amphibolite, epidote-amphibolite and rarely in greenschist facies conditions.

The Gvadra suite includes micaceous metapelites, migmatites, and paragneisses, as well as meta-igneous amphibole schist and amphibolites. Gukasyan & Somin (1995) reported seven whole-rock Rb–Sr analyses of mica schist from the Gvandra suite, which they used to obtain isochron ages of 655±28 and 316±27 Ma. Somin et al. (2007) used U–Pb dating (SHRIMP) of zircon from quartz–biotite schist in the Gvandra suite to identify four zircon age groups (2394–1929, 669–483, 425–405 and 355–325 Ma), the first three of which they interpreted as detrital, while the last group – as magmatic and metamorphic ages.

The Klichi suite consists mainly of amphibolites with intercalations of amphibole- and biotite-schists. $^{207}Pb/^{206}Pb$ dating of zircons from the amphibolite of the Klichi suite yielded an age of 600±20 Ma (Hanel et al. 1993a,b).

The Sissina suite comprises mainly metapelites with minor amphibolite bodies.

Magmatic rocks are an important component of the Buulgen complex, with pre-Alpine trondhjemites, gabbro-diorites, diorites, quartz-diorites and leucocratic granitoids (predominantly alaskites) confined to this complex. Among these rocks

the Sakeni, Klichi and Sgimazuk intrusives should be noted (Fig. 2).

The Sakeni intrusive (ca. 70 km²) is a low-K, I-type trondhjemite to quartz diorite intrusion in the Buulgen complex, which hosts numerous intrusives of such composition (Fig. 2). Shengelia et al. (2014) identified two populations of ages in the Sakeni intrusive using U–Pb LA–ICP–MS analyses of zircon: one Concordia age at 325.3±2.5 Ma associated with the Variscan orogeny (with epidote-amphibolite and low temperature part of amphibolites facies) and a second at 658–603 Ma representing xenocrystic zircons of Cadomian age captured by granitoids.

The Klichi intrusive, which differs from the Klichi metasedimentary suite described above, consists of hornblende gabbros to diorite orthogneisses in the lower part of the Buulgen complex (Fig. 2), with orthogneisses yielding a concordant Variscan age of 320 Ma (Bibikova et al. 1991).

In the Sgimazuk intrusive, the Gvandra and Klichi suites of the Buulgen complex are extensively intruded by pre-Variscan granites that are both concordant with, and cross-cutting (Okrostsvaridze et al. 2000; Gamkrelidze & Shengelia 2005). These suites are cut also by Variscan sodic granites and orthogneisses (Okrotsvaridze et al. 2000; Okrotsvaridze & Tormay 2011) (Fig. 2).

The Gvandra suite includes concordant and cross-cutting bodies of Variscan granitoids (granites, granodiorites, alaskites and aplites (Shengelia et al. 1978; Somin 2011). They indicate that the magmatic rocks in the Buulgen complex were intruded at the end of the Devonian and in the Middle-Late Carboniferous, and were then metamorphosed together with their host rocks during a single Variscan regional metamorphism.

However, the overwhelming majority of research on the crystalline core of the GC has convincingly demonstrated a regional metamorphic event that took place prior to the intrusion of Variscan granite, as indicated by the cross-cutting relations (e.g., cutting and capture of crystal schists by host intrusions) (Shengelia 1972; Baranov & Kropachov 1976; Baranov et al. 1977; Belov et al. 1978). Two specific types of cross-cutting relations contradict a single magmatic and metamorphic event. The first is about xenoliths. Both the Klichi and Sakeni intrusions contain xenoliths that were highly metamorphosed prior to the Variscan (Fig. 3). The second phenomenon is the contact effect of the Klichi and Sakeni intrusives on the rocks of the Gwandra Formation, which were previously metamorphosed at a peak temperature of 620 °C (Gamkrelidze & Shengelia 2005).

Orthogneiss of the Klichi intrusive has a concordant Variscan age of 320 Ma (Bibikova et al. 1991).

The Laba metamorphic complex

The Laba metamorphic complex comprises four allochthonous units (Adamia 1984; Gamkrelidze & Shengelia 2005): Mamkhurts, Damkhurts, Lashtrak, and Adjarka. The metavolcanic to meta-sedimentary Damkhurts unit contains carbonate layers with Siluro–Devonian fossils and polymict stretched-pebble conglomerates with diverse pebble compositions notably lacking quartzite (Somin 2011). The Adjarka unit contains quartzite, amphibolite, porphyry, and fossiliferous limestones (Somin 2011) with post-Ordovician crinoids (Potapenko & Stukalina 1971). With the Adjarka nappe are spatially closely related so-called Beshta and Kamenistaia intrusives consisting of oceanic type granites (Shengelia et al. 1989; Okrostsvaridze 1990) (Fig. 2).

The Elbrus sub-zone

The Elbrus sub-zone can be subdivided into two units: the Gondarai complex, which comprises mainly autochthonous

Fig. 3. Variscan Sakeni granitoid of the Pass sub-zone along the river Sakeni hosting xenoliths that were highly metamorphosed prior to the Variscan orogeny (Shengalia 1972).

basement (i.e., the infrastructure) and the overlying, overthrust from the Pass sub-zone before the emplacement of Variscan granitoids, the Makera nappe (Gamkrelidze et al. 1996), or suprastructure (Baranov & Kropachov 1976).

Gondarai metamorphic complex (Infrastructure)

The Gondarai complex consist of migmatites, crystalline schists, with rare intercalation of pre-Variscan ortho- and paragneisses, as well as of porphyroblastic and equigranular granitoids. Two stages of regional metamorphism have been established: a Pre-Variscan high temperature event at amphibolite to sub-granulite facies conditions (590–720 °C, P=2.6–2.8 kbar), and a lower grade Variscan event at epidote-amphibolite to greenschist facies conditions (440–510 °C, C<1.5 kbar) as determined via thermobarometry (Shengelia et al.1977; Kaneko & Miyano 2004; Wu et al. 2004; Powel & Holland 2008) and analysis of trends in the temperature and pressure conditions of regional metamorphism in the GC (Korikovsky et al. 1991).

Somin et al. (2007) and Somin (2011) report single-grain U–Pb (SHRIMP) analyses of zircons from the Gondarai metamorphic complex that yielded both Variscan and pre-Variscan ages. But these authors believe that all the pre-Variscan zircons are detrital.

The latter include ages of 425±9 Ma from a concordant population of five grains in a gabbro amphibolite that cuts orthogneiss; 637 and 665 Ma from paragneiss; 675 to 561 Ma from six grains in another paragneiss; 670, 660, and 645 Ma from metasedimentary schist; 634 to 522 Ma from foliated and slightly migmatized rocks; 676–560 Ma and 504–474 Ma from sillimanite–garnet paragneiss; 400±10 and 386±10 Ma from orthogneiss; and 425±6 Ma from gabbro cutting the orthogneiss (Somin 2011).

Intrusive complexes of biotite-granodiorite gneisses (orthogneisses) are wide-spread in the Gondarai complex. Hanel et al. (1993a) obtained a Pb–Pb age of 500±40 Ma from zircons from two samples of these rocks, which they interpreted as the protolith age, and an age of 540±40 Ma from an augen gneiss in the Gondarai complex, which they interpreted also as the protolith age. U–Pb dating of magmatic zircons from orthogneiss in the Adil-Su intrusive, in the upper reaches of the Baksan River, yielded an age of ca. 400 Ma (Somin 1991). From synmetamorphic orthogneisses of three different massifs of the Gondarai complex by SHRIMP, the group of ages 420–460 Ma was obtained (Gerasimov et al. 2010). It should be especially noted that Somin et al. (2007) in Adil-Su orthogneiss of Caledonian (Ordovician) age note the presence of xenoliths of metamorphic rocks: paragneisses and amphibolites of country rocks. According to Gamkrelidze & Shengalia (2005) in the same orthognesses there are xenoliths of paragneisses, migmatites, biotitized amphibolites and crystal schists. These xenoliths of metamorphic rocks in Caledonian orthogneisses most likely indicate the manifestation of Cadomian regional metamorphism confirmed by the newest geochronological data (see below).

The latest stage of development in the Elbrus sub-zone was intrusion of Variscan porphyroblastic and equigranular two-mica granites (i.e. "Ullukam-type" granites), with which are associated diaphtoresis and hydrothermal mineralization (Korikovski 1991).

Ullukam-type granites contain abundant xenoliths of highly metamorphosed rocks (Fig. 4).

Within the Gondarai complex, the oldest K–Ar dates are 330±15 Ma (muscovite) and 325±15 Ma and 323±8 Ma (biotite) in pegmatoids located in porphyroblastic granites, 317±23 Ma (muscovite) in muscovite–microcline pegmatites (Shengelia 1972), and 321±6 Ma in muscovite pegmatites rock from the Dariali massif (Dudauri et al. 2000) (Fig. 2). U–Pb LA–ICP–MS analyses of zircons from the Dariali massif yielded two age groups: 316–304 Ma, associated with the Variscan orogeny, and 690–629 Ma associated with xenocrystic Cadomian zircons apparently engulfed by Variscan granite (Shengelia et al. 2014).

Makera nappe

As noted above, the Makera nappe is overthrust from south to north and comprises most of the Sissina suite of the Buulgen complex, although in places the nappe also includes small parts of the underlying Klichi suite (Gamkrelidze et al. 1996) (Fig. 2).

Overthrusting of the Makera nappe took place during the Early Variscan (Bretonian) orogeny (seemingly in the Turneasian), which corresponds to the most important pre-Alpine time of nappe formation in the Caucasus as a whole. In this time the most important developments were dynamic events, especially processes of tectonic layering of the Earth's crust, its shortening and accretion of terranes (Gamkrelidze et al. 1996).

The Makera nappe mainly consists of metapelitic rocks and amphibolites, the protoliths of which were various terrigenous deposits with rare intercalations of basic rocks.

A number of Pre-Variscan dates have been reported from different rocks within the Makera nappe.

Andalusite schist yielded SHRIMP ages of 605–546 Ma and 524–444 Ma (Somin 2011). Metapelitic rocks yielded dates of 487±5 Ma by classical U–Pb and 462±8 Ma by $^{86}Sr/^{87}Sr$ analysis (Somin et al. 2007). Amphibolite yielded a SHRIMP age of 460±8 Ma (Somin et al. 2007). U–Pb (SHRIMP) analysis of orthoamphibolite and orthogneiss yielded ages of 445±12 Ma and 430–470 Ma, respectively (Somin et al. 2007; Somin 2011). Somin et al. (2004) used U–Pb analyses of zircon from amphibolites to obtain dates of 553±31 and 460±8 Ma, which they interpret as the ages of protolith crystallization and regional metamorphism, respectively. However, as noted above, in their subsequent work (Bibikova et al. 1991; Somin 2011) all Pre-Variscan dates without any reasoning are presented as detrital.

In summary, geological, petrological, and previous geochronological data in our opinion suggest at least two stages of regional metamorphism in the Pass and Elbrus sub-zones of the MR GC: an earlier Pre-Variscan and Variscan.

Fig. 4. Xenoliths of pre-Variscan, highly metamorphosed rocks within equigranular, two mica Ullukam-type Variscan granites of the Elbrus sub-zone in the river Chegemi (Shengelia 1972)..

To investigate the older Pre-Variscan event, we used single-grain U–Pb LA–ICP–MS analysis of zircon from both the Gvandra suite of the Buulgen metamorphic complex and the Klichi and Sgimazuk granitoid intrusive complexes in the Pass sub-zone, as well as the Gondarai complex of the Elbrus sub-zone.

Analytical methods

Zircon grains were extracted using standard crushing/sieving, magnetic, and heavy liquid separation techniques and then hand picked under a binocular microscope. They were mounted in epoxy together with grains of the standard material, polished, and then imaged using reflected and transmitted light and cathodoluminescence imaging. Single-grain U–Pb dating of zircon was conducted at the National Chung-Cheng University, Taiwan using an Agilent 7500s quadrupole ICP–MS equipped with a New Wave UP213 laser ablation system. Laser spots were positioned based on zoning patterns observed in the CL images. Calibration was performed using either the GJ-1 zircon standard (Jackson et al. 2004) or the Plešovice zircon (Sláma et al. 2008). All U–Th–Pb isotope ratios were calculated using GLITTER 4.4.2 (GEMOC) software, and the isotope ratio of common lead was corrected using the approach of Andersen (2002). We used Isoplot v. 3.0 (Ludwig 2003) to calculate weighted mean U–Pb ages, determine probability density curves, and to produce Concordia plots. For details of the analytical procedure and data accuracy, see Knittel et al. (2014) and Chiu et al. (2009). Mineral abbreviations follow Whitney & Evans (2010) and are listed in increasing order of abundance.

Results

The zircons investigated here are morphologically and optically heterogeneous and CL images indicate that most crystals

contain relict cores overgrown with later rims (Fig. 5 and Supplementary Figs. S1 and S3). Consequently, these different zones encode the ages of different events. Here we report 406 individual analyses from 387 different grains from a total of 14 samples, with 7 each from the Pass and Elbrus sub-zones. Specifically, in the Pass sub-zone, we analysed 1 orthogneiss from the Klichi intrusive (sample N1), 3 meta-sedimentary rocks from the Gvandra suite of the Buulgen complex (samples N2, N3, and N4), and 3 magmatic rocks from the Sgimazuk intrusive complex (samples GE15, GE17, and GE18). In the Elbrus sub-zone all 7 samples are from the Gondarai complex, 4 of which are igneous or meta-igneous rocks (samples 1Z, 4Z, 5Z, and 7Z), with the remaining 3 being meta-sedimentary migmatite rocks (samples 2Z, 3Z, and GE30). Sample locations are shown in Fig. 2. Single-grain

results are detailed in Supplementary Tables S1 and S2 and in probability density curves and Concordia diagrams (Figs. 6 and 8 as well as Supplementary Figs. S2 and S4). Table 1 summarizes U–Pb zircon ages of the MR GC as a whole.

The Pass sub-zone

Sample N1 is gabbro-diorite orthogneiss from the Klichi intrusive (Fig. 2). 39 spots on 30 grains were analysed. Th/U=0.18 to 0.54. The weighted mean age is 310.9±2.4 Ma (MSWD=1.2; Supplementary Fig. S2). Note that in three cases (Supplementary Fig. S1 and Table S1) dates from the cores of zoned crystals are younger than those from the rims by 2, 5 and 10 Ma.
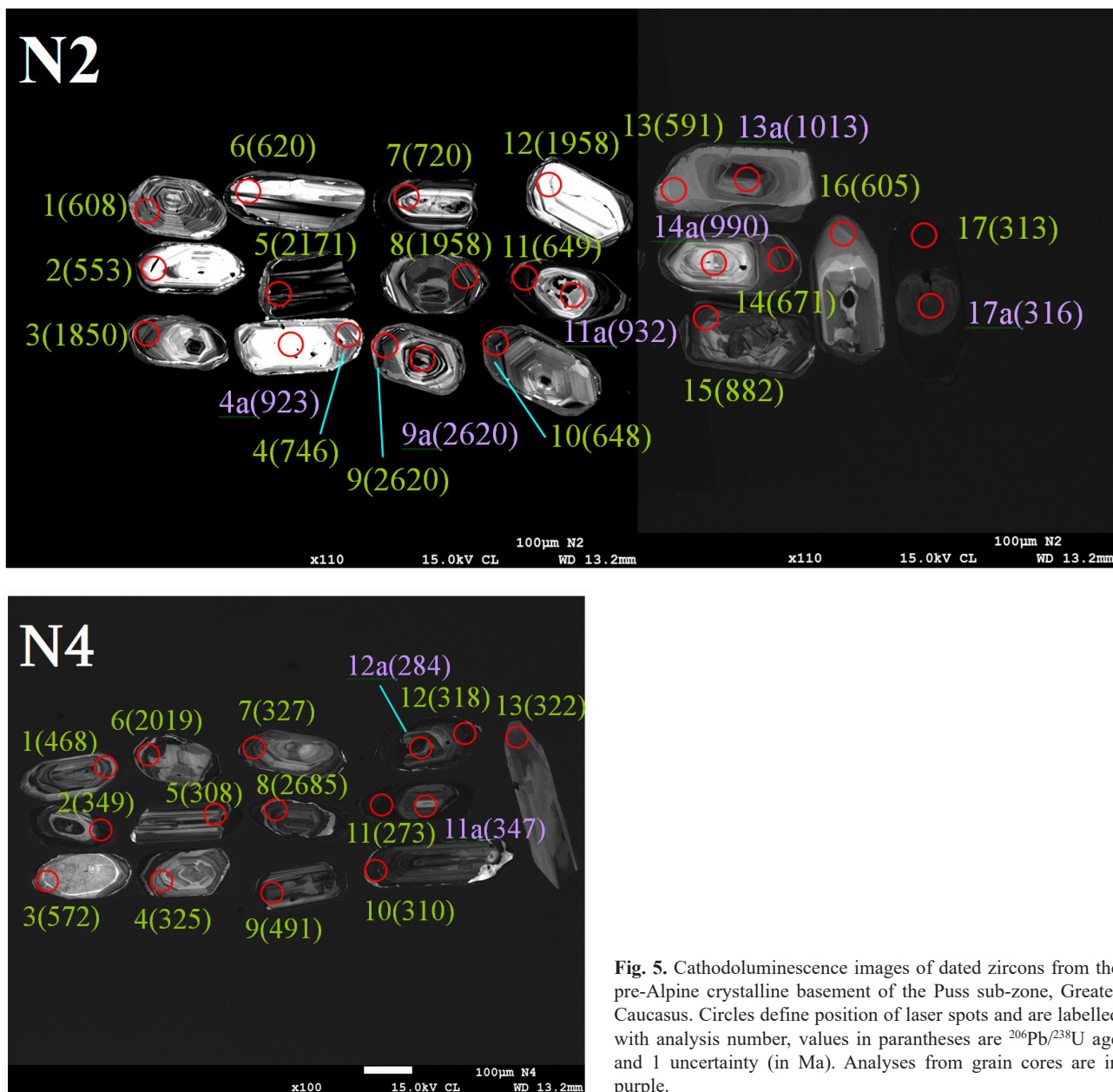
Fig. 5. Cathodoluminescence images of dated zircons from the pre-Alpine crystalline basement of the Puss sub-zone, Greater Caucasus. Circles define position of laser spots and are labelled with analysis number, values in parantheses are ^{206}Pb/^{238}U age and 1 uncertainty (in Ma). Analyses from grain cores are in purple.
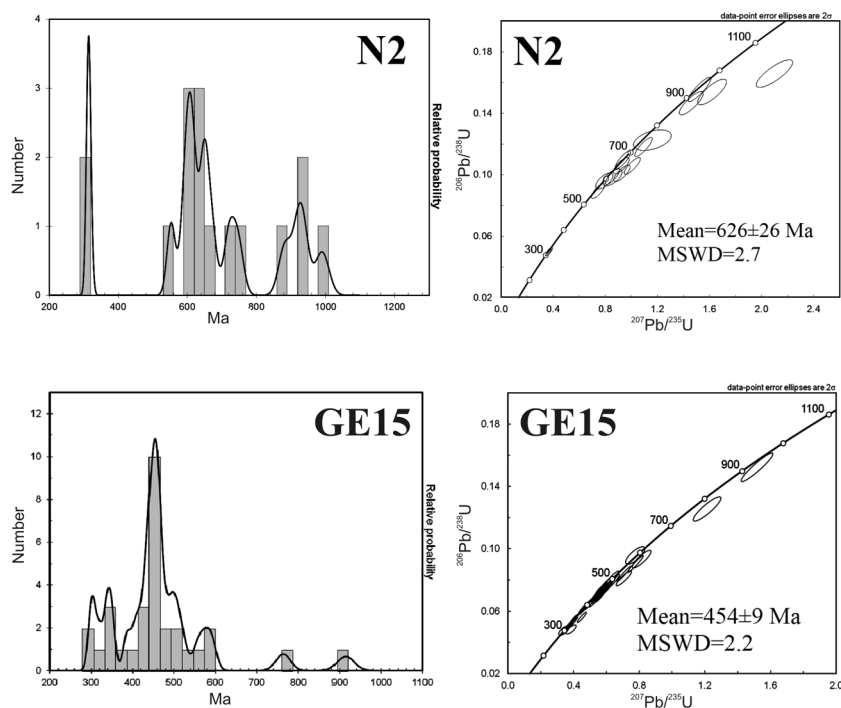
Fig. 6. Probability density curves for the analysed zircons and Concordia diagrams for samples from the Pass sub-zone of the Greater Caucasus.

Sample N2 is a metapelitic Grt–Bt–Pl–Qtz schist from the Gvandra suite of the Buulgen metamorphic complex in the Gvandra river gorge (Fig. 2). 23 spots on 17 grains are analysed. Th/U=0.08 to 1.23. The weighted mean age is 626±26 Ma (MSWD=2.7; Fig.6).

Sample N3 is a metapelitic Grt–Andl–Bt–Ms–Qtz–Pl schist from the Gvandra Suite of the Buulgen complex in the Khetskvsra river gorge (Fig. 2). 12 spots on 10 grains are analysed. Th/U=0.17 to 0.39. The weighted mean age is 312.5± 4 Ma (MSWD=1.15; Supplementary Fig. S2).

Sample N4 is a metapelitic Grt–Bt–Andl±Sil–Pl–Ms–Qtz schist from the Gvandra suite of the Buulgen complex in the Ptishi river gorge (Fig. 2). 15 spots on 13 grains are analysed. Th/U=0.16 to 0.69. The weighted mean age is 317.0 ±8.3 Ma (MSWD=1.4; Fig. 6). In one case the date from the core of a zoned crystal is younger than the rim by 34 Ma (Fig. 5 and Supplementary Table S1).

Sample GE15 is a laminated orthogneiss from the Zgimazuk intrusive complex (Fig. 2). 32 grains (1 spot/grain) are analysed. Th/U=0.04 to 0.87. The weighted mean age is 454 ±9 Ma (MSWD=2.2; Fig. 6).

Sample GE17 is from a leucocratic 60 cm thick granite body, which represents the last phase of the Zgimazuk intrusive complex (Fig. 2). 27 grains (1 spot/grain) are analysed. Th/U=0.01 to 0.93. The weighted mean age is 309±8 Ma (MSWD=2.8; Supplementary Fig. S2).

Sample GE18 is from a 3.5 m thick alaskite body from the last phase of the Zgimazuk intrusive complex. 28 spots on 28 grains are analysed. Th/U=0.11 to 0.76. The weighted mean age is 325±4 Ma (MSWD=1.3; Supplementary Fig. S2).

The Elbrus sub-zone

Sample 1Z is from a granite orthogneiss with Bt+Pl+Kfs+Qtz and a horizontal extent of 2.5 km in the Gondarai complex along the western tributary of the Nenskra river (Fig. 2). 33 grains (1 spot/grain) are analysed. Th/U=0.01 to 1.08. The weighted mean age is 468±5 Ma (MSWD=0.76; Fig. 8).

Sample 2Z is from a two-mica Bt+Ms+Pl+Qtz meta-sedimentary 2 m thick migmatite body in the Gondarai metamorphic complex along the Memuli river (western tributary of the Neneskra river) (Fig. 2). 26 grains (1 spot/grain) were analysed. Th/U=0.056 to 0.064. The weighted mean age is 461±5.3 Ma (MSWD=1.04; Fig. 8).

Sample 3Z is from a Grt–Bt+Ms+Pl+Qtz meta-sedimentary 2.5 m thick migmatite body in the Gondarai complex along the Memuli river (Fig. 2). 27 grains (1 spot/grain) have been analysed. Th/U=0.1 to 1.22. The weighted mean age is 627±19Ma (MSWD=2.44; Fig. 8).

Sample 4Z is from a gnessic Bt+Pl+Kfs+Qtz 0.5 m thick granite vein that is concordant with migmatite in the Gondarai complex, also along the Memuli river (Fig. 2). 39 grains (1 spot/grain) were analysed. Th/U=0.01 to 0.57. The weighted mean age is 471.7±4.6 Ma (MSWD=1.05; Fig. 8).

Sample 5Z is from a Bt+Pl+Qtz trondhjemite gneiss that is exposed for over 2.7 km within the Gondarai complex along the Nenskra river gorge (Fig. 2). 47 grains (1 spot/grain) were analysed. Th/U=0.00 to 1.20. The weighted mean age is 357±5.9 Ma (MSWD=2,6; Supplementary Fig. S4).

Sample 7Z is from an Ulukam-type equigranular granite intrusion with an exposed area of 32 km² in the Gindarai

complex along the Sakeni river gorge (Fig. 2). 30 grains (1 spot/grain) were analysed. Th/U=0.00 to 1.20. The weighted mean age is 311±4.9 Ma (MSWD=1.3; Supplementary Fig. S4).

Sample GE30 is from a Grt+Bt+Sil+Pl+Qtz meta-sedimentary 500 m thick migmatite body in the Gondarai complex along the Sakeni river gorge (Fig. 2). 27 grains (1 spot/grain) were analysed. Th/U = 0.01 to 0.56. The weighted mean age is 457 ±12 Ma (MSWD=2.0; Fig. 8)

All the results cited above are summarized in the Table 1.

Discussion

The zircon analyses reported here from the crystalline basement of the GC reveal both zircons formed within the GC and those transported from outside the region. We interpret all zircons older than 650 Ma (i.e., the beginning of the Cadomian orogeny) as detrital exotic grains that have been transported from areas outside the Caucasus region because these ages are singular and scattered. Besides, according to geological data pre-Cadomian endogenic processes have not been established
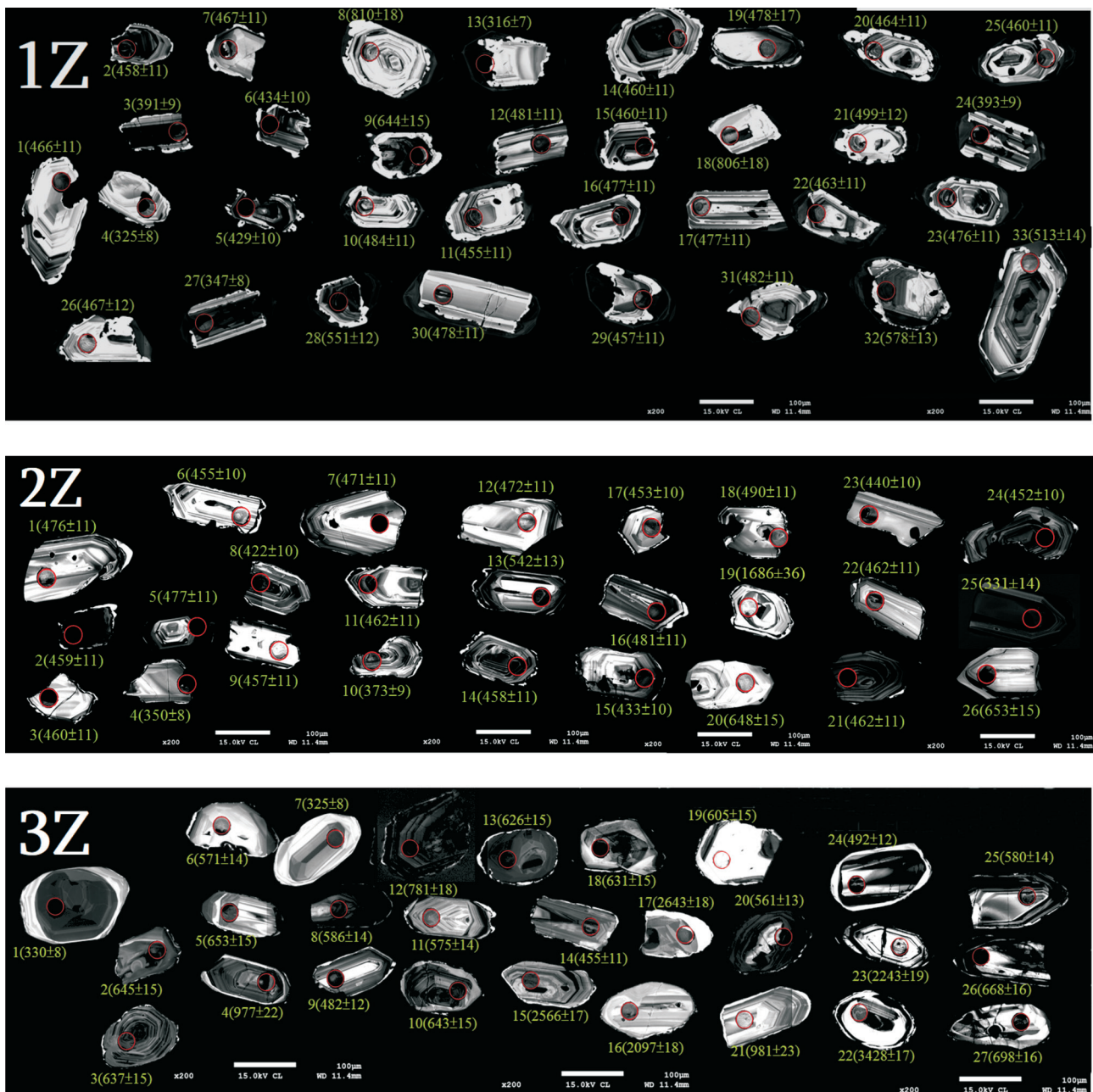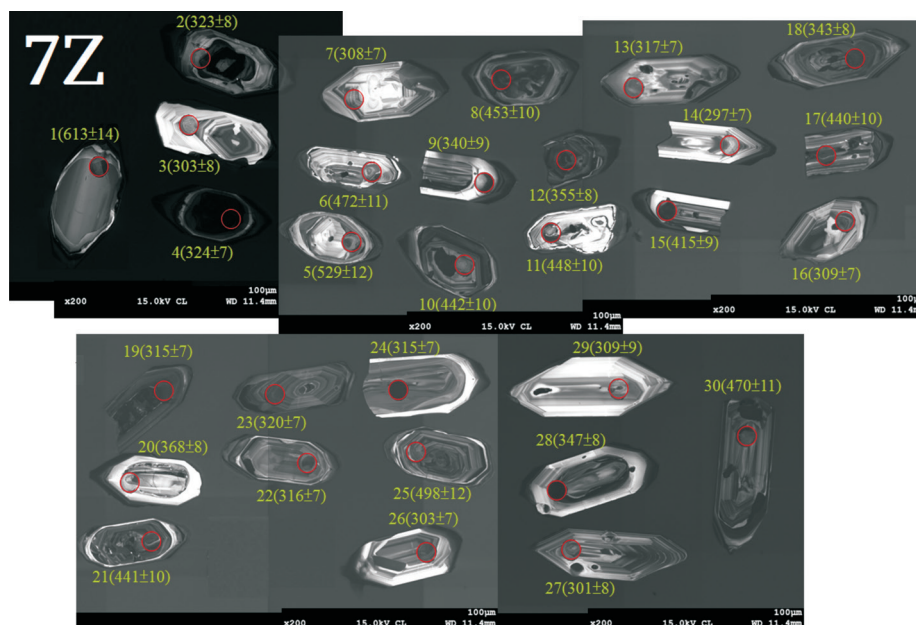

Fig. 7. Cathodoluminescence images of dated zircons from pre-Alpine basement of the Elbrus sub-zone, Greater Caucasus. Symbols same as in Fig. 5.

Fig. 7 (continued). Cathodoluminescence images of dated zircons from pre-Alpine basement of the Elbrus sub-zone, Greater Caucasus. Symbols same as in Fig. 5.

in the GC region. The ages of these detrital zircons range from 3428 to 668 Ma. It is noteworthy that cores of a number of detrital zircons, evidently already located in the GC, with younger rims, including rims of Cadomian age (650–550 Ma) are overgrown (Fig. 5: sample N2, crystals 1, 2, 10, 11, 13 and 16; Fig. 7: sample 1Z, crystals 9 and 32; sample 2Z, crystals 13 and 20; sample 3Z, crystals 3, 10, 11, 13 and 20). Besides, Caledonian (Ordovician) figures (490–390 Ma) very often from the rims of zircon crystals are also obtained (Fig. 5: sample N 4, crystal 1 and 9; Fig. 7: sample 1Z, crystals 5, 6, 10, 14, 16, 17, 20, 23, 31 and 26; sample 2Z, crystals 2, 5, 6, 11, 14, 15 and 24). Such cases can also be seen for samples 4Z and GE30 in Electronic Supplement.

Pre-Cadomian detrital zircons of the GC before the Early Paleozoic time could have come from the south – from the Black Sea–Central Transcaucasian terrane (microcontinent), basement of which in the Neoproterozoic was composed of highly metamorphosed rocks (Gamkrelidze & Shengelia 2005; Gamkrelidze et al. 2011), and possibly from the north, from the Scythian platform where the Riphean crystalline basement was recently discovered at great depth (Bush 2014). Later, in the Paleozoic time, after the formation of small oceanic basins, to the north and south of the GC (Gamkrelidze & Shengelia 2005), these zircons were evidently repeatedly redeposited from older formations or captured by Paleozoic granitoids.

Several age groups have been recorded among in situ zircons in different zones of zoned crystals. As noted above in the Pass sub-zone in some cases (in samples N4 and N1) the cores of crystals are sufficiently younger than the rims. According to Gerdes & Zeh (2009) such phenomena indicate that some zircon rims were less affected by Pb-loss than the core domains.

According to weighted mean age data in the Pass sub-zone of the MR GC zircons with ages of 626±2 Ma (Sample N2) and 454±9 Ma (Sample GE15) are found, the first of which was obtained from the meta-sedimentary rocks of the Buulgen metamorphic complex, and the second from the Zgimazuk granitoid intrusive complex. In addition, here in the meta-sedimentary rocks of the Buulgen complex, zircons with ages of 312.5±4 Ma and 317.0±8.3 Ma were detected (Samples N3 and N4), and in the meta-igneous rocks of the Klichi and Zgimazuk granitoid intrusions – 309±8 Ma, 310.9±2.4 Ma and 325±4 Ma (samples GE17, N1 and GE18, respectively).

The first figure – 626±2 Ma corresponds to the manifestation of the earliest – Cadomian stage of high temperature regional metamorphism (T=530–630 °C, P=3.2–3.4 kbar). For this time we have no evidence of magmatic activity. Although it is possible that serpentinous ultrabasic and gneissic basic intrusive rocks, that are developed in both sub-zones of the Greater Caucasus, are Cadomian, they do not contain zircons.

In the Pass sub-zone, unlike the Elbrus sub-zone, we obtained only a few separate figures, corresponding to the Caledonian regional metamorphism. However, as noted above, Somin et al. (2004) obtained from the meta-sedimentary rocks of the Buulgen complex age figures in the range 425–405 Ma, which, in our opinion they unreasonably attributed to detrital zircons. In addition, in the Makera complex, which, according to our data, is overthrust from the Pass subzone, Somin et al. (2007) obtained from metapelitic rocks by classical U–Pb analysis 462±8 Ma and from amphibolites – 460±8 Ma, which they earlier (Somin et al. 2004) interpreted as the age of regional metamorphism. Thus, based on these data, we consider it possible to allow the manifestation of the Caledonian regional metamorphism in the Pass subzone.
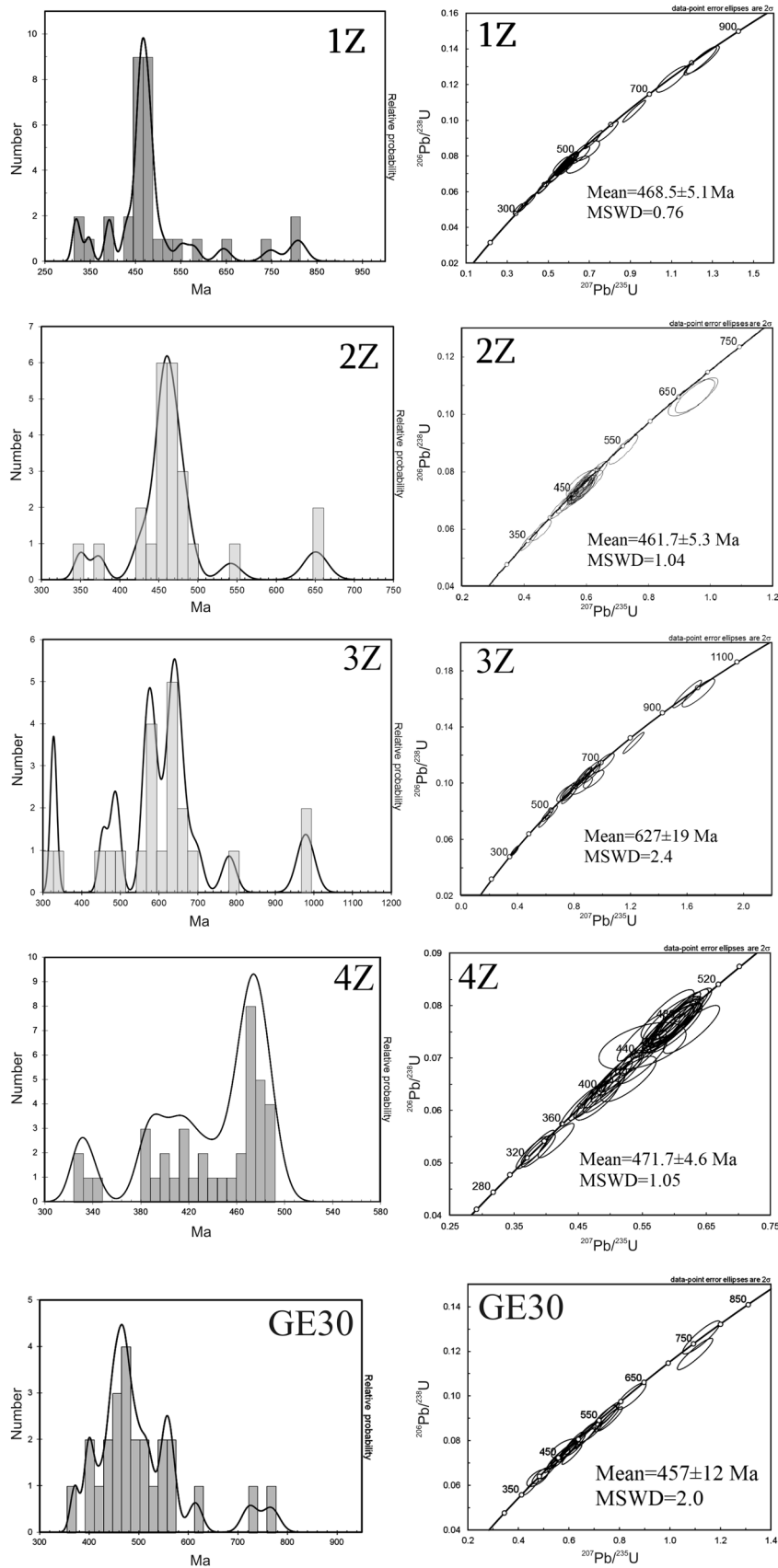
Fig. 8. Probability density curves for the analysed zircons and Concordia diagrams for samples from the Elbrus sub-zone of the Greater Caucasus.

Table 1: Summary of U–Pb zircon ages of the Main Range zone of the Greater Caucasus.

Sample number	Lithology	Sample location and coordinates	Mean Concordia age of zircons from the meta-sedimentary (ms) and magmatic (m) rocks						Number of spots
			Sub-zone	Unit	Variscan	Caledonian	Cadomian	Exotic (more than 650 Ma)	
N1	orthogneiss	gorge of the Klichi river 41°51'45"N, 43°10'32"E	Pass	Klichi intrusive	310.9±2.4 Ma (m) MSWD=1.2	–	–	–	39
N2	metapelitic schist	gorge of the Gvandra river 41°53'04"N, 43°07'48"E	Pass	Gvandra suite Buulgen Complex	–	–	626±26 Ma (ms) MSWD=2.7	2620–671 (12)	23
N3	metapelitic schist	gorge of the Khetskvara river 41°45'32"N, 43°09'41"E	Pass	Gvandra suite Buulgen Complex	312.5±4 Ma (ms) MSWD=1.15	–	–	–	12
N4	metapelitic schist	gorge of the Ptishi river 41°42'21"N, 43°10'02"E	Pass	Gvandra suite Buulgen Complex	317.9±8.3 Ma (ms) MSWD=1.4	–	–	2685–2019 (2)	15
GE15	orthogneiss	gorge of the Tsaneri river 42°54'33"N, 43°03'27"E	Pass	Zgimasuk intrusive complex	–	454±9 Ma (m) MSWD=2.2	–	2603–914 (2)	32
GE17	granite	gorge of the Tsaneri river 42°54'19"N, 43°03'20"E	Pass	Zgimasuk intrusive complex	309±8 Ma (m) MSWD=2.8	–	–	–	27
GE18	alaskite	gorge of the Tsaneri river 42°54'13"N, 43°02'45"E	Pass	Zgimasuk intrusive complex	325±4 Ma (m) MSWD=1.3	–	–	–	28
1Z	orthogneiss	gorge of the Nenskra river 42°15'10"N, 43°09'06"E	Elbrus	Gondarai complex	–	468.5±5.1 Ma (m) MSWD=1.15	–	810–806 (2)	33
2Z	meta-sedimentary migmatite	gorge of the Nenskra river 42°11'43"N, 43°07'38"E	Elbrus	Gondarai complex	–	461.7±5.3 Ma (m) MSWD=1.04	–	1686	26
3Z	meta-sedimentary migmatite	gorge of the Nenskra river 42°11'44"N, 43°07'39"E	Elbrus	Gondarai complex	–	–	627±19 Ma (ms) MSWD=2.4	2981–668 (10)	27
4Z	gneissic granite	gorge of the Nenskra river 42°11'44"N, 43°07'40"E	Elbrus	Gondarai complex	–	471.7±4.6 Ma (m) MSWD=1.05	–	–	39
5Z	trondhjemite gneiss	gorge of the Nenskra river 42°14'26"N, 43°08'36"E	Elbrus	Gondarai complex	357.2±5.9 Ma (m) MSWD=2.6	–	–	2232–733 (7)	47
7Z	equigranular granite	gorge of the Nenskra river 42°14'26"N, 43°08'37"E	Elbrus	Gondarai complex	311.6±4.9 Ma (m) MSWD=1.3	–	–	–	30
GE30	meta-sedimentary migmatite	gorge of the Sakeni river 42°25'56"N, 42°30'04"E	Elbrus	Gondarai complex	–	457±12 Ma (ms) MSWD=2.0	–	2662–724 (4)	27

The figure – 454±9 Ma, obtained by us from the Zgimazuk granitoid inrusive complex, corresponds to apparently syn-metamorphic granitoid formation in the Pass sub-zone associated with the Caledonian orogeny.

As noted above, the next – Early Variscan (Bretonian) orogeny (seemingly in Turneasian), corresponds to the time of nappe formation in the Caucasus as a whole. In this time dynamic events were the most important. In particular, fleeting processes of tectonic layering of the Earth's crust, its shortening and accretion of terranes. It was precisely the time when the Makera metamorphic complex of the Pass sub-zone was overthrust onto the Elbrus sub-zone.

The third age group of zircons (312.5±4 and 317.0± 8.3 Ma) corresponds to the Late Variscan regressive regional metamorphism (T=440–510 °C, P<1.2–1.8 kbar). And the fourth age group (309±8 Ma, 310.9 Ma and 325±4 Ma) reflects the syn-metamorphic Late Variscan Granitoid activity in the Pass sub-zone of the GC.

In the Elbrus sub-zone of the MR GC, from the meta-sedimentary rocks of the Gondarai metamorphic complex, the following figures were obtained: 1) 627±19 Ma (sample 3Z), which corresponds to Cadomian high temperature regional metamorphism (T=650–750 °C, P=3 kbar), which is preserved only as small fragments, since its associations were transformed because of Caledonian metamorphism; 2) 461±5.3 Ma (sample 2Z), 457±12 Ma (sample GE30), which corresponds to Caledonian regional metamorphism (T=500–620 °C, P=3 kbar); 3) 468±5 Ma and 471.7±4.6 Ma (samples 1Z and N4), obtained from the metagranitoid rocks of the Gondarai complex, corresponding to Caledonian synmetamorphic magmatic activity; 4) 311±5.9 Ma and 357± 5.9 Ma (samples 7Z and GE30) from the granitoids of the Gondarai complex, corresponding to Variscan apparently synmetamorphic granitoid formation.

In the Elbrus sub-zone in meta-sedimentary rocks, unlike the Pass sub-zone, ages of Variscan regional metamorphism

were obtained only as a few separate figures and weighted mean ages are absent. However, Somin (2011) from paragneiss of the Gondarai complex by the SHRIMP method mark the Concordia age of Variscan metamorphism 321±1 Ma. There are also many K/Ar determinations of Variscan age in synmetamorphic granitoid rocks of the sub-zone (Somin et al. 2007). Based on this, we assume the manifestation of Variscan regional metamorphism in the Elbrus sub-zone.

As regards the values for Th/U, which are usually seen as a criterion for the determination of the formation of zircon in igneous or metamorphic conditions, it requires special consideration. In our case, they have variable, but mostly larger than 0.1 values, which indicate igneous origin. But such high values are also found in meta-sedimentary rocks (for example Cadomian, Caledonian and Variscan zircons in samples N2, N3, N4, 3Z and GE30 where Th/U is in the range of 0.1–1.3). At the same time, it is clear that Variscan zircons, which have rather high values of Th/U (0.16–0.69) cannot be detrital or igneous in these older deposits and are very likely to have metamorphic origins. We do not exclude that many other zircon grains, despite the relatively high value of Th/U, are also metamorphic. The fact is that according to plenty of authors in many cases metamorphic zircons recorded average and high Th/U (from 0. 15 to 3.2 – Pidgeon 1992; Vavra et al. 1999; Bingen et al. 2001; Harley et al. 2001; Carson et al. 2002; Moller et al. 2002, 2003; Hokada & Harley 2004; Hokada et al. 2004; Kelly & Harley 2005; Gagnevin et al. 2010; Kaulina 2010; Krosnobaev &Valizer 2015 etc.).

Thus according to the aforesaid within the pre-Alpine basement of the GC, the Th/U method in many cases cannot give an unambiguous answer about the genesis of zircons. Especially interpretation of the values of Th/U as >0.1 comes into conflict with geological facts. In particular, as stated above, with the presence of xenoliths of metamorphic rocks both in Variscan and in Caledonian granitoids.

We share the opinion that the concentrations of Th and U in zircon are primarily dependent on the presence of an element in the crystallization medium and the distribution of Th and U between zircon and coexisting minerals, melts and fluids (Kaulina 2010).

The opinion about the universality of this approach to determining the genesis of zircons is sometimes erroneous, and without taking into account geological and petrological data, it can cause serious errors in the geodynamic interpretation of isotope ages (Moller et al. 2002).

As a matter of fact, Th/U, as for magmatic zircon, should reflect primarily the composition of the source (melt or fluid) from which zircon crystallizes, and not the temperature conditions of metamorphism. For example, in granulites of the Ivrea zone (Southern Alps) the Th/U in zircon increases with the degree of metamorphism from low values in zircons of the upper limit of the amphibolite facies to medium and high in zircon from the rocks of the transition zone and granulite facies, respectively (Vavra et al. 1999).

The new radiometric isotope data, side by side with existing geological, petrological and some previous geochronological

data, contradict the opinion about the manifestation of only one – Variscan stage of regional metamorphism in the GC as believed Bibikova et al. (1991), Somin at al. (2007), Somin (2011). It should also be noted that this interpretation of the history of metamorphism is also contradicted by the following fact: the Late Variscan metamorphism, having a regressive character everywhere, with maximal temperature 510 °C cannot form such rocks as amphibolite or sub-granulite and high temperature amphibolite facies, with brown hornblende and ortho- and clinopyroxene, crystalline schist, with silimanite and cordierite, and migmatite (Shengelia 1968; Baranov & Kropachov 1976; Perchuk et al. 1984). These rocks are widespread in the MR GC and were formed at the temperature interval from 650 to 750 °C.

In addition, the natural question arises here: if all pre-Variscan zircons are detrital (exotic), then how can we explain the existence of identical age groups of zircons and peaks of their ages in completely different parts of the GC, coinciding in the overwhelming majority of cases, along with Variscan, with Caledonian and Kadomian orogenies? Moreover, their manifestation is confirmed by geological data (see Figs. 3 and 4).

And finally, it is very important that from the Early Paleozoic, the MR GC was isolated from the continental masses of the Scythian plate in the north and the Black Sea–Central Transcaucasian terrane in the south accordingly by small oceanic basins of Arkhiz and the Southern slope of the GC (Gamkrelidze & Shengelia, 2005), and throughout the Paleozoic, before the closing of these basins at the end of the Paleozoic and at the beginning of the Mesozoic, the GC could not have received any material including external zircons.

Thus, within both sub-zones of Main Range zone of the GC new geochronological data (International Chronostratigraphic Chart 2019) indicate the manifestation of endogenous activity associated with Cadomian, Caledonian and Late Variscan orogenies.

Identification of the Cadomian regional metamorphism in the Buulgen complex of the Pass sub-zone and Gondarai complex of the Elbrus sub-zone points apparently to the Precambrian (Cryogenian) age of parent rocks of these complexes.

In should be noted that on the basis of the afore-cited new results of radiometric isotope dating, along with geological and paleomagnetic data and age of ophiolites, we can re-examine the pre-Alpine tectonic evolution of the GC and adjacent areas, but this will be the subject of a separate paper.

Conclusions

• Using the new U–Pb dating of the pre-Alpine basement of the GC constituent rocks several age groups of zircons have been identified. Both detrital zircons, and those formed within the Greater Caucasus have been revealed. Ages of detrital zircons range from 2981 to 668 Ma.

- According to weighted mean age data among in situ zircons from both sub-zones of the MR GC the first age group: 626±2 Ma and 627±19 Ma correspond to the earliest – Cadomian stage of high temperature regional metamorphism.
- The second age group: 461±5.3 Ma, 457±12 reflects the Caledonian stage of high temperature prograde regional metamorphism in the Elbrus sub-zone.
- In granitoid rocks of both sub-zones the third age group of figures: 454±9 Ma, 468±5 Ma and 471.7±4.6 Ma corresponds to the Caledonian stage of synmetamorphic granitoid formation.
- The next – Early Variscan (Bretonian) orogeny (seemingly in the Turneasian), corresponds to the most important pre-Alpine time of nappe formation in the Caucasus as a whole. It was at this time that the Makera nappe from the Pass sub-zone was overthrust onto the Elbrus sub-zone.
- The fourth age group of zircons: 312.5±4 Ma, 317.0±8.3 Ma corresponds to Late Variscan regressive regional metamorphism in the Pass sub-zone.
- The fifth age group of zircons – 309±8 Ma, 310.9 Ma, 325±4 Ma, 311±5.9 Ma and 357±5.9 Ma corresponds to Late Variscan stage of synmetamorphic granitoid formation.
- Identification of the Cadomian regional metamorphism in the Buulgen complex of the Pass sub-zone and Gondarai complex of the Elbrus sub-zone of the MR GC points apparently to the Precambrian (Cryogenian) age of parent rocks of these complexes.

These conclusions are in good agreement with the geological and petrological data on the MR GC.

References

Adamia S. 1984: Pre-Alpine basement of the Caucasus – composition, structure, formation. In: Tectonics and metallogeny of the Caucasus. *Metsniereba,* 1–104 (in Russian).

Adamia S., Zakariadze G., Chkhotua T. & Sadradze N. 2011: Geology of the Caucasus: A.Review. *Turkish Journal of Earth Sciences.* 20. 489-544. https://doi.org/10.3906/yer-1005-11

Andersen T. 2002: Correction of common lead in U–Pb analyses that do not report [204]Pb. *Chem. Geol*. 192, 59–79. https://doi.org/10.1016/S0009-2541(02)00195-X

Baranov G. & Kropachov S. 1976: Stratigraphy, magmatism and tectonics of the Greater Caucasus Precambrian and Paleozoic stages. *Nedra,* Moscow, 1–212 (in Russian).

Baranov G., Grekov I. & Dolgikh A. 1977: Explanatory note to the map of the Greater Caucasus metamorphism and magmatism. *Sevkavkazgeologia*, 1–39 (in Russian).

Belov A., Somin M. & Adamia S. 1978: Precambrian and Paleozoic of the Caucasus (brief synthesis). *Jahrbuch der Geologische Bundesanstalt* 121, 1, 155–175.

Bessonov I. 1938: Geological–petrological features of the Bolshoi and Mali Zelenchuk river-heads. *Proceedings on geology and mineral resourses of the North Caucasus* 1, 55-–96 (in Russian).

Bibikova E., Somin M., Krasivskaia I., Grachev T., Makarov V., Arakeliants M. & Vidiapin I. 1991: U–Pb age of orthogneisses of the Main Range of the Greater Caucasus. *Izvestia AN SSSR, Ser. Geol.* 9, 23–34 (in Russian).

Bingen B., Austrheim H. & Whitehouse M. 2001: Ilmenite as a source for zirconium during high-grade metamorphism? Textural evidence from the Caledonides of Western Norway and implications for zircon geochronology. *J. Petrol.* 42, 2, 355–375. https://doi.org/10.1093/petrology/42.2.355

Bush V. 2004: The deep structure of the Scythian plate. *Geotectonics* 48, 6, 415–426.

Carson C., Ague J. & Coath C. 2002: U–Pb geochronology from Tonagh Island, East Antarctica:implications for the timing of ultra-high temperature metamorphism in the Napier Complex. *Precambrian Res.* 116, 237–263. https://doi.org/10.1016/S0301-9268(02)00023-2

Chiu, H.Y., S. L. Chung, F. Y. Wu, D. Liu, Y. H. Liang, I. J. Lin, Y. Iizuka, L. W. Xie, Y. Wang, and M. F. Chu, 2009: Zircon U–Pb and Hf isotopic constraints from eastern Transhimalayan batholiths on the precollisional magmatic and tectonic evolution in southern Tibet. *Tectonophysics* 477, 3–19. https://doi.org/10.1016/j.tecto.2009.02.034

Dudauri O., Tsimakuridze G., Vashakidze G. & Togonidze M. 2000: New data on the age of the Dariali massif. *Proceedigs of Janelidze Institute of Geology of Georgian Acad. of Sci., New Ser*. 115, 306–310 (in Russian).

Gagnevin D., Stephan Daly J. & Kronz A. 2010: Zircon texture and chemical composition as a guide to magmatic processes and mixing in a granitic environment and coeval volcanic system. *Contrib. Mineral. Petrol.* 159, 559–596. https://doi.org/10.1007/s00410-009-0443-0

Gamkrelidze I. 1997: Terranes of the Caucasus and adjacent areas. *Bull. Georg. Acad. Sci.* 155, 3, 75–81.

Gamkrelidze I. & Shengelia D. 2005: Precambrian–Paleozoic regional metamorphism, granitoid magmatism and geodynamics of the Caucasus. *Nauchni Mir*, Moscow, 1–458 (in Russian with an extensive English summary).

Gamkrelidze I. & Shengelia D. 2007: Pre-Alpine geodynamics of the Caucasus, suprasubduction regional metamorphism and granitoid magmatism. *Bull. Georg. Acad. Sci*. 175, 1, 57–65.

Gamkrelidze I., Shengelia D. & Chichinadze G. 1996: Makera nappe in the crystalline core of the Greater Caucasus and its geological significance. *Bull. Georg. Acad. Sci*. 154, 1, 84–89.

Gamkrelidze I., Shengelia D., Tsutsunava T., Sun-Lin Chung, Han-Vichin & Chikhelisze K. 2011: New data on the U–Pb zircon age of the pre-Alpine basement of the Black Sea-Cenrtal Transcaucasian terrane and their geological significance. *Bull. Georg. Acad. Sci*. 5, 1, 64–76.

Gerasimov V. I., Pismenni A.N. & Enna N.L. 2010: Zirconometry of meta-granitods of crystallinicum of the Greater Caucasus. In: Magmatism and metamorphism in history of the Earth, 2. *Petersburg University Publishing*, 167–168 (in Russian).

Gerdes A. & Zeh A. 2009: Zircon formation versus zircon alteration – new insights from combined U-–Pb and Lu–Hf in-situ LA-ICP-MS analyses, and consequences for the interpretation of Archean zircon from the Central zone of the Limpopo Belt. *Chem. Geol*. 261, 230–243. https://doi.org/10.1016/j.chemgeo.2008.03.005

Grekov I. & Lavrishchev V. 2002: On nomenclature, correlation and age of metamorphic complexes of the Greater Caucasus. In: Problems of geology, mineral resources and ecology in Southern Russia and The Caucasus. *Edition of Novocherkask University* 2, 49–58 (in Russian).

Gukasian R. & Somin M. 1995: Rb–Sr izochrone dating of metamorphic rocks of the Main Range of the Caucasus. In: Materials of VIII Iubilee Conference on geology snd mineral resources of the North Caucasus. *Sevkavkaz Publishing*, 239–240 (in Russian).

Hanel M., Lippold H., Kober B. & Gurbanov A. 1993a: Izotope-geochemical reconstruction of protolites of volcanic rocks in metamorphic complexes of the Greater Caucasus. *Petrologia* 1, 171–188 (in Russian).

Hanel M., Lippold H., Kober B. & Gurbanov A. 1993b: On Early Paleozoic age of metagranitoids on the Main Range of the Greater Caucasus. *Petrologia* 5, 487–498 (in Russian).

Harley S., Kinny P., Snape I. & Black L. 2001: Zircon chemistry and the definition of events in Archaean granulite terrains. In: Fourth International Archaean Symposium, Extended Abstract Volume. *AGSO Geoscience Australia Record* 37, 511–513.

Hokada T. & Harley S. 2004: Zircon growth in UHT leucosome: constraints from zircon–garnet rare earth element (REE) relations in Napier Complex, East Antarctica. *Journal of Mineralogical and Petrological Sciences* 99, 180–190. https://doi.org/10.2465/jmps.99.180

Hokada T., Misawa K., Yokoyama K., Shiraishi K. & Yamaguchi A. 2004: SHRIMP and electron microprobe chronology of UHT metamorphism in the Napier Complex,Eastern Antarctica: implication for zircon growth at >1000 °C. *Contrib. Mineral. Petrol.* 147, 1–20. https://doi.org/10.1007/s00410-003-0550-2

International Chronostratigraphic Chart 2017: *International Comission of Stratigraphy, IUGS.*

Jackson S.E., Pearson N.J., Griffin W.L. & Belousova E.A. 2004: The application of laser ablation-inductively coupled plasma-mass spectrometry to in situ U–Pb zircon geochronology. *Chem. Geol.* 211, 47–69. https://doi.org/10.1016/j.chemgeo.2004.06.017

Kaneko Y. & Miyano T. 2004: Recalibration of mutually consistent garnet–biotite and garnet–cordierite geothermomether. *Lithos* 73, 255–269. https://doi.org/10.1016/j.lithos.2003.12.009

Kaulina T. 2010: Formation and recrystallization of zircon in polimetamorphic complexes. *Edition of Koli peninsula Scientific Centre*, 1–144 (in Russian).

Kelly N. & Harley S. 2005: An integrated microtextural and chemical approach to zircon geochronology: refining the Archaean history of the Napier Complex, East Antarctica. *Contrib. Mineral. Petrol.* 149, 57–84. https://doi.org/10.1007/s00410-004-0635-6

Knittel U., Suzuki S., Nishizaka N., Kimura K., Tsai W.L., Lu H.Y., Ishikawa Y., Ohno Y., Yanagida M. & Lee Y.H. 2014: U–Pb ages of detrital zircons from the Sanbagawa Belt in western Shikoku: Additional evidence for the prevalence of Late Cretaceous protoliths of the Sanbagawa Metamorphics. *J. Asian Earth Sci.* 96, 148–161. https://doi.org/10.1016/j.jseaes.2014.09.001

Korikovski S. 1991: Retrogade metamorphism of the Hercynian cycle. In: Petrology of metamorphic complexes of the Greater Caucasus. *Nauka*, Moscow, 210–212 (in Russian).

Korikovsky S., Shengelia D. & Somin M. 1991: Model of pre-Alpine zoned metamorphism of the Greater Caucasus. In: Petrology of the Metamorphic Complexes of the Greater Caucasus. *Nauka*, Moscow, 216–222 (in Russian).

Krasnobaev A. & Valizer P. 2015: Zirconology of garnet schists of the Maksyutov complex (Southern Urals). *Doklady Earth Sciences* 461, 2, 414–418. https://doi.org/10.1134/S1028334X15040212

Lebedko G. & Usik A. 1985: Geochronology of the North Caucasus. *Edition of Rostov University*, 19–30 (in Russian).

Ludwig K.R. 2003: User's manual for Isoplot 3.00: a geochronological toolkit for Microsoft Excel, *Kenneth R. Ludwig*.

Möller A., O'Brien P., Kenned A. & Kröner A. 2002: Polyphase zircon in ultratemperature granulites (Rogaland, SW Norway): constrains for Pb diffusion in zircon. *J. Metamorph. Geol.* 20, 727–740. https://doi.org/10.1046/j.1525-1314.2002.00400.x

Möller A., O'Brien P., Kennedy A. & Kröner A. 2003: Linking growth episodes of zircon and metamorphic textures to zircon chemistry: an example from the ultrahigh temperature granulites of Rogaland (SW Norway). *Geol. Soc. London, Spec. Publ.* 220, 65–81.

Okrotsvsridze A. 1990: granitogneisses of tholeiitic series of the Main Range zone of the Greater Caucasus. *Doklady AN SSSR* 314, 1, 234–236 (in Russian).

Okrostsvaridze A. 2007: Herzynian granitoid magmatism of the Greater Caucasus. *Proceedings of Janelidze Institute of Geology, new ser.* 123, 1–223 (in Russian).

Okrostsvaridze A., Mgaloblishvili J. & Bluashvili D. 2000: Plagiogranites of Szgimazuki massif and ore manifestation related to it. *Bull. Acad. Georg. Sci.* 162, N1, 116–119.

Okrostsvaridze A. & Tormay D. 2011: Evolution of the Variscan orogenic plutonic magmatism: The Greater Caucasus. *Journal of Nepal Geological Society* 43, Spec. Iss., 45–52.

Perchuk L.L., Lavrent'yeva I.V., Kotel'nikov A.R. & Petrík I. 1984: Comparative characteristics of thermodynamic regimes of metamorphism of the rocks of the Main Caucasian Range and the Western Carpathians. *Geol. Carpath.* 35, 1, 105–155.

Pidgeon R.T. 1992: Recrystallization of oscillatory zoned zircon: some geochronological and petrological implications. *Contrib. Mineral. Petrol.* 110, 463–472. https://doi.org/10.1007/BF00344081

Potapenko Y. & Stukalina G. 1971: The first discovery of fossils in a metamorphic complex of the Main Range of the Greater Caucasus. *Doklady Earth Science*s 198, 1161–1162 (in Russian).

Powell R. & Holland J. 2008: On thermobarometry. *J. Geol.* 26, 155–179. https://doi.org/10.1111/j.1525-1314.2007.00756.x

Rubinstein M. 1970: Regional and local rejuvenation of Argon on example of the Caucasus. *Eclogae Geol. Helv.* 63, 1, 281–289 (in German).

Shengelia D. 1968: Granulitic facies of the Greater Caucasus. *Izvestia AN SSSR, Ser. Geol.* 7, 23–33 (in Russian).

Shengelia D. 1972: Petrology of Paleozoic granitoids of the North Caucasus. *Proceedings of Janelidze institute of geology of Acad. of sci. of Georgian SSR*, 34–46 (in Russian).

Shengelia D., Akhvlediani R. & Ketskhoveli D. 1977: Graphitic thermometer. *Doklady AN SSSR* 235, 6, 1407–1410 (in Russian).

Shengelia D., Ketskhoveli D. & Chichinadze G. 1978: Paleozic leucocrate garnet gneisses and granitoids of Abkhazia. In: Problems of geology of Georgia. *Proceedings of institute of geology of Acad. of Sci. of Georgian SSR*, *New Ser.* 59, 147–159 (in Russian).

Shengelia D., Chichinadze L. & Okrostsvaridze A V. 1989: New data on plagiogranitogneisses of Beshta and Mountain Kamenistaia. *Akad. Sciences of Georgian SSR* 135, 2, 393–396 (in Russian).

Shengelia D.M., Korikovsky S.P., Chichinadze G.L., Kakhadze R., Somin M.L., Potapenko V.Y., Okrotsvaridze A. & Poporadze N. 1991: Petrology of the Metamorphic Complexes of the Greater Caucasus. *Nauka*, Moscow, 1–232 (in Russian).

Shengelia D.M., Korikovsky S.P., Chichinadze G.L., Kakhadze R., Somin M.L., Potapenko V.Y., Okrotsvaridze A. & Poporadze N. 1995: Metamorphic facies of the Greater Caucasus. *Metsniereba,* Tbilisi (in Russian).

Shengelia D., Tsutsunava T., Chichinadze G. & Beridze G. 2014: Some questions on structure, Variscan regional metamorphism and granitoid magmatism of the Greater Caucasian terrane. *Bull. Georg. Acad. Sci.* 11, 1, 56–63.

Sláma J., Košler J., Condon D.J., Crowley J.L., Gerdes A., Hanchar J.M., Horstwood M.S.A., Morris G.A., Nasdala L., Norberg N., Schaltegger U., Schoene B., Tubrett M.N. & Whitehouse M.J. 2008: Plešovice zircon – A new natural reference material for U–Pb and Hf isotopic microanalysis. *Chem. Geol.* 249, 1–35. https://doi.org/10.1016/j.chemgeo.2007.11.005

Somin M. 1971: Pre-Jurassic basement of the Main Range and Southern Slope of the Greater Caucasus. *Nauka*, Moscow, 1–245 (in Russian).

Somin M. 1991: Geological characteristic of metamorphic complexes of the Greater Caucasus. In Petrology of the Metamorphic Complexes of the Greater Caucasus. *Nauka,* Moscow, 8–45 (in Russian).

Somin M.L. 2011: Pre-Jurassic basement of the Greater Caucasus: brief overview. *Turkish J. Earth Scie.* 20, 3–65. https://doi.org/10.3906/yer-1008-6

Somin M., Bayanova T., Levkovich N. & Lavrishevich V. 2004: Geological and geochronological study of the basement of the Main Range of the Greater Caucasus: new data and problems. *Proceedingns of Janelidze Institute of Geology of Georgian Acad. of Sci. New Ser.* 119, 521–534 (in Russian).

Somin M., Lepekhina E. & Konilov A. 2007: Age of the high-temperature gneiss core of the Central Caucasus. *Doklady Earth Sciences* 415, 690–694.

Vavra G., Shmid R. & Gebauer D. 1999: Internal morphology, habit and U–Th–Pb microanalysis of amphibolite-to-granulite facies zircons: Geochronology of the Ivrea Zone (Southern Alps). Contrib. Mineral. Petrol. 134. 380–404. https://doi.org/10.1007/s004100050492

Whitney D. & Evans B. 2010: Abbreviations for names of rock-forming minerals. *Am. Mineral.* 95, 185–187. https://doi.org/10.2138/am.2010.3371

Wu C., Zhang J. & Ren L. 2004: Empirical garnet–biotite–plagioclase–quatrtz (GBPQ) geobarometry in medium to high-grade metapelites. *J. Petrol.* 45, 9, 1907–1921. https://doi.org/10.1093/petrology/egh038

Zaridze G. & Shengelia D. 1978: Hercynian magmatism and metamorphism of the Great Caucasus in the light of plate tectonics. *Bulleten de la Societe Geologique France* XX, 3, 355–359.

Supplement

Table S1: LA–ICP–MS zircon U–Pb isotopic analytical data of sample N1–N4 and GE15, GE17, GE18. The letter "a" with the number of sample indicates that these age figures are obtained from the core of zircon crystals and the remaining figures are from the rim of crystals.

N1											
Spot	Th/U	U ppm	$^{207}Pb/^{206}Pb$	1σ	$^{207}Pb/^{235}U$	1σ	$^{206}Pb/^{238}U$	1σ	error corr	Inferred age (Ma)	1σ
N1-1	0.36	560	0.05393	0.00062	0.37903	0.00985	0.05098	0.00108	0.815194572	321	7
N1-1a	0.47	527	0.0518	0.00061	0.3676	0.00973	0.05147	0.00109	0.800082907	324	7
N1-2	0.48	688	0.054	0.00062	0.37179	0.00968	0.04994	0.00106	0.815229101	314	7
N1-2a	0.43	527	0.05328	0.00065	0.36457	0.00989	0.04963	0.00106	0.787310832	312	7
N1-3	0.30	347	0.05336	0.00072	0.37728	0.01088	0.05128	0.00109	0.737077865	322	7
N1-3a	0.45	433	0.05669	0.0008	0.39453	0.01166	0.05048	0.00106	0.710506411	317	7
N1-4	0.37	414	0.05356	0.0007	0.38929	0.01102	0.05272	0.00112	0.750471621	331	7
N1-5	0.51	70	0.05035	0.00167	0.34855	0.0185	0.05021	0.0012	0.450281789	316	7
N1-6	0.45	459	0.05231	0.00059	0.36076	0.00926	0.05002	0.00106	0.825599782	315	7
N1-7	0.34	352	0.05187	0.00182	0.35119	0.0178	0.0491	0.00107	0.429956406	309	7
N1-8	0.39	313	0.05261	0.00067	0.34622	0.00965	0.04774	0.00102	0.76655372	301	6
N1-9	0.38	285	0.0538	0.00071	0.3651	0.01036	0.04923	0.00104	0.744484364	310	6
N1-10	0.37	146	0.0615	0.0009	0.58194	0.01779	0.06863	0.00147	0.700657213	428	9
N1-11	0.18	432	0.05158	0.0006	0.34921	0.00917	0.04911	0.00104	0.806456118	309	6
N1-12	0.39	303	0.05114	0.00066	0.35291	0.00994	0.05005	0.00107	0.75902709	315	7
N1-13	0.47	342	0.05325	0.00067	0.35071	0.00971	0.04777	0.00101	0.763651224	301	6
N1-14	0.42	427	0.05299	0.00064	0.35395	0.00947	0.04845	0.00102	0.786861557	305	6
N1-15	0.45	357	0.05186	0.00065	0.35024	0.00969	0.04899	0.00104	0.767304715	308	6
N1-16	0.34	199	0.05179	0.00081	0.34298	0.01095	0.04803	0.00104	0.678227554	302	6
N1-17	0.34	180	0.05414	0.00087	0.37394	0.01225	0.0501	0.0011	0.670225264	315	7
N1-17a	0.46	158	0.05383	0.00087	0.37045	0.01219	0.04992	0.00111	0.675731704	314	7
N1-18	0.38	258	0.05269	0.00072	0.35064	0.0103	0.04827	0.00105	0.740519046	304	6
N1-19	0.38	156	0.05268	0.00085	0.35872	0.01185	0.04939	0.0011	0.67420334	311	7
N1-20	0.44	271	0.05598	0.00078	0.39481	0.01193	0.05116	0.00116	0.750369467	322	7
N1-21	0.35	396	0.05197	0.00063	0.34433	0.00933	0.04805	0.00103	0.791110323	303	6
N1-20a	0.44	447	0.05251	0.00062	0.35913	0.00956	0.0496	0.00106	0.802819628	312	7
N1-22	0.46	363	0.0556	0.00069	0.36724	0.0101	0.04791	0.00103	0.781699184	302	6
N1-23	0.25	249	0.054	0.00076	0.37004	0.01108	0.0497	0.00109	0.73245175	313	7
N1-24	0.25	315	0.05375	0.00073	0.35184	0.01028	0.04749	0.00102	0.735106223	299	6
N1-24a	0.42	416	0.05363	0.00067	0.35845	0.00994	0.04848	0.00104	0.773593707	305	6
N1-25	0.34	744	0.05227	0.00056	0.36208	0.00888	0.05024	0.00106	0.860295805	316	7
N1-26	0.43	407	0.05345	0.00064	0.35416	0.00942	0.04805	0.00102	0.798096463	303	6
N1-27	0.36	293	0.05516	0.00069	0.39153	0.01085	0.05148	0.0011	0.771062271	324	7
N1-28	0.54	662	0.05327	0.00059	0.37122	0.0093	0.05055	0.00107	0.844911139	318	7
N1-28a	0.43	240	0.0524	0.00127	0.37336	0.01672	0.05168	0.00134	0.57899366	325	8
N1-29	0.31	527	0.053	0.00062	0.37257	0.0098	0.05098	0.00107	0.797931762	321	7
N1-29a	0.34	398	0.05162	0.00194	0.35813	0.01887	0.05032	0.0011	0.414878429	316	7
N1-30	0.30	411	0.05283	0.00066	0.35956	0.00989	0.04936	0.00105	0.773373396	311	6
N1-30a	0.36	255	0.0521	0.00076	0.35857	0.01096	0.04992	0.00107	0.701249554	314	7

N2											
Spot	Th/U	U ppm	$^{207}Pb/^{206}Pb$	1σ	$^{207}Pb/^{235}U$	1σ	$^{206}Pb/^{238}U$	1σ	error corr	Inferred age (Ma)	1σ
N2-1	0.63	224	0.06278	0.00073	0.85644	0.02256	0.09895	0.00215	0.824860503	608	13
N2-2	0.78	236	0.06038	0.00076	0.74547	0.02093	0.08956	0.002	0.795384005	553	12
N2-3	0.36	269	0.12572	0.00127	5.76251	0.1337	0.33249	0.00712	0.922957473	1850	34
N2-4	0.39	178	0.06872	0.00241	1.16177	0.05924	0.12262	0.00273	0.436622833	746	16
N2-4a	0.62	102	0.07632	0.00096	1.62001	0.04532	0.15398	0.00342	0.793943477	923	19
N2-5	0.37	751	0.15935	0.00162	8.79701	0.20457	0.40043	0.00854	0.917116283	2171	39
N2-6	1.05	167	0.06668	0.00084	0.92856	0.0259	0.10102	0.00221	0.7843233	620	13
N2-7	0.12	394	0.06716	0.00074	1.09392	0.02738	0.11816	0.00253	0.855464826	720	15
N2-8	1.37	346	0.12009	0.00126	5.10129	0.12297	0.30811	0.00653	0.879201109	1958	19

Table S1 (continued): LA–ICP–MS zircon U–Pb isotopic analytical data of sample N1–N4 and GE15, GE17, GE18. The letter "a" with the number of sample indicates that these age figures are obtained from the core of zircon crystals and the remaining figures are from the rim of crystals.

							N2				
Spot	Th/U	U ppm	$^{207}Pb/^{206}Pb$	1σ	$^{207}Pb/^{235}U$	1σ	$^{206}Pb/^{238}U$	1σ	error corr	Inferred age (Ma)	1σ
N2-9	0.55	246	0.17647	0.00187	10.0818	0.24426	0.4144	0.00885	0.881473477	2620	17
N2-9a	0.94	378	0.17644	0.00188	9.85016	0.24057	0.40494	0.00854	0.863513256	2620	18
N2-10	0.52	206	0.06906	0.00077	1.00731	0.02549	0.1058	0.00225	0.840407966	648	13
N2-11	0.08	405	0.0632	0.00081	0.92319	0.02493	0.10594	0.00217	0.758522693	649	13
N2-12	1.15	149	0.12013	0.00122	4.69372	0.10898	0.2834	0.0059	0.896649149	1958	18
N2-11a	0.39	333	0.07098	0.00073	1.52303	0.03602	0.15563	0.00326	0.885704869	932	18
N2-13	1.23	78	0.05986	0.00102	0.79274	0.02693	0.09605	0.00213	0.65279475	591	13
N2-13a	1.20	210	0.07297	0.00078	1.71334	0.04184	0.17032	0.00361	0.86794745	1013	21
N2-14	0.02	258	0.06184	0.00069	0.93577	0.02383	0.10976	0.00234	0.837176125	671	14
N2-14a	0.40	101	0.09174	0.00111	2.09855	0.05713	0.16593	0.00368	0.81466302	990	20
N2-15	0.54	177	0.07222	0.00082	1.4605	0.03754	0.14668	0.00312	0.827543793	882	18
N2-16	0.56	62	0.06301	0.00115	0.85415	0.03063	0.09832	0.00224	0.635321126	605	13
N2-17	0.01	1370	0.05317	0.00058	0.36433	0.00906	0.0497	0.00105	0.849570936	313	6
N2-17a	0.03	551	0.05347	0.00065	0.3709	0.01	0.05031	0.00107	0.788835222	316	7

							N3				
Spot	Th/U	U ppm	$^{207}Pb/^{206}Pb$	1σ	$^{207}Pb/^{235}U$	1σ	$^{206}Pb/^{238}U$	1σ	error corr	Inferred age (Ma)	1σ
N3-1	0.35	291	0.05056	0.00077	0.36456	0.01141	0.0523	0.00113	0.690335371	329	7
N3-2	0.39	429	0.05219	0.00066	0.35333	0.00972	0.04911	0.00103	0.762397633	309	6
N3-2a	0.13	3280	0.05244	0.00052	0.3595	0.00823	0.04973	0.00102	0.895943807	313	6
N3-3	0.31	477	0.05273	0.00071	0.36512	0.01063	0.05023	0.00109	0.745359306	316	7
N3-4	0.31	318	0.05387	0.00074	0.3609	0.01059	0.0486	0.00103	0.722257196	306	6
N3-5	0.28	296	0.05314	0.00076	0.35735	0.01074	0.04878	0.00104	0.709383444	307	6
N3-6	0.17	418	0.05354	0.00067	0.39112	0.01077	0.05299	0.00111	0.760717453	333	7
N3-7	0.35	100	0.05195	0.00149	0.34882	0.01659	0.04871	0.00112	0.483453696	307	7
N3-8	0.23	199	0.05572	0.00088	0.46722	0.01493	0.06083	0.0013	0.668785969	381	8
N3-9	0.21	165	0.05367	0.00099	0.37045	0.01315	0.05007	0.0011	0.618897802	315	7
N3-10	0.35	49	0.05379	0.00258	0.37361	0.02598	0.05039	0.00128	0.365296034	317	8
N3-10a	0.31	657	0.05778	0.00067	0.66654	0.01741	0.08368	0.00175	0.800652056	518	10

							N4				
Spot	Th/U	U ppm	$^{207}Pb/^{206}Pb$	1σ	$^{207}Pb/^{235}U$	1σ	$^{206}Pb/^{238}U$	1σ	error corr	Inferred age (Ma)	1σ
N4-1	0.37	471	0.05686	0.00064	0.59094	0.01492	0.07538	0.00155	0.814423187	468	9
N4-2	0.16	455	0.05227	0.00061	0.40147	0.01049	0.05571	0.00118	0.810637068	349	7
N4-3	0.03	83	0.0628	0.00099	0.80303	0.0261	0.09275	0.00206	0.68335215	572	12
N4-4	0.38	328	0.05281	0.00068	0.37664	0.01058	0.05174	0.00111	0.763725564	325	7
N4-5	0.27	736	0.05291	0.00064	0.35669	0.00966	0.0489	0.00107	0.807957889	308	7
N4-6	0.12	489	0.1243	0.00134	5.64853	0.14638	0.32958	0.00693	0.811383332	2019	19
N4-7	0.37	422	0.05747	0.00069	0.41253	0.01107	0.05206	0.00111	0.79456006	327	7
N4-8	0.78	801	0.18348	0.00185	12.04421	0.27891	0.47614	0.00997	0.904221281	2685	17
N4-9	0.10	492	0.05738	0.0007	0.62626	0.01687	0.07917	0.00164	0.768993722	491	10
N4-10	0.69	1138	0.05199	0.00058	0.35352	0.0089	0.04932	0.00104	0.837595342	310	6
N4-11	0.01	2591	0.05163	0.00056	0.30783	0.00758	0.04325	0.00091	0.854470389	273	6
N4-11a	0.31	455	0.05169	0.00067	0.39447	0.0111	0.05537	0.00117	0.750934988	347	7
N4-12	0.27	775	0.05268	0.00057	0.36723	0.00909	0.05057	0.00106	0.846812346	318	7
N4-12a	0.18	2664	0.05241	0.00054	0.32494	0.00761	0.04498	0.00093	0.88284003	284	6
N4-13	0.21	525	0.05344	0.00063	0.37673	0.00987	0.05114	0.00107	0.798612506	322	7

Table S1 (continued): LA–ICP–MS zircon U–Pb isotopic analytical data of sample N1–N4 and GE15, GE17, GE18. The letter "a" with the number of sample indicates that these age figures are obtained from the core of zircon crystals and the remaining figures are from the rim of crystals.

GE15											
Spot	**Th/U**	**U ppm**	**^{207}Pb/ ^{206}Pb**	**1σ**	**^{207}Pb/ ^{235}U**	**1σ**	**^{206}Pb/ ^{238}U**	**1σ**	**error corr**	**^{206}Pb/^{238}U age (Ma)**	**1σ**
GE15-1	0.27	202	0.0723	0.0008	1.5179	0.0395	0.1523	0.0037	0.9393	914	21
GE15-2	0.31	204	0.0575	0.0007	0.5687	0.0159	0.0717	0.0018	0.8821	447	11
GE15-4	0.87	215	0.0630	0.0008	0.7052	0.0194	0.0812	0.0020	0.8951	503	12
GE15-5	0.56	252	0.0571	0.0007	0.5605	0.0156	0.0712	0.0018	0.8856	443	11
GE15-6	0.23	839	0.0553	0.0007	0.4924	0.0135	0.0646	0.0016	0.9177	404	10
GE15-7	0.04	1130	0.0541	0.0006	0.3985	0.0104	0.0534	0.0013	0.9392	335	8
GE15-10	0.69	88	0.0521	0.0010	0.3414	0.0129	0.0475	0.0012	0.6821	299	8
GE15-11	0.30	957	0.0530	0.0006	0.3706	0.0100	0.0508	0.0012	0.9091	319	8
GE15-12	0.11	2275	0.0609	0.0007	0.7054	0.0175	0.0840	0.0020	0.9757	520	12
GE15-13	0.44	47	0.1791	0.0020	12.2848	0.3120	0.4975	0.0121	0.9553	2603	52
GE15-14	0.24	1654	0.0578	0.0006	0.5301	0.0133	0.0666	0.0016	0.9647	415	10
GE15-15	0.80	119	0.0577	0.0009	0.3836	0.0127	0.0483	0.0012	0.7614	304	8
GE15-16	0.17	253	0.0568	0.0007	0.5686	0.0158	0.0726	0.0018	0.8850	452	11
GE15-18	0.52	146	0.0632	0.0008	0.8144	0.0233	0.0935	0.0023	0.8629	576	14
GE15-19	0.06	1095	0.0569	0.0007	0.6064	0.0172	0.0773	0.0018	0.8330	480	11
GE15-20	0.47	192	0.0700	0.0009	1.2130	0.0343	0.1256	0.0032	0.8887	763	18
GE15-21	0.30	233	0.0569	0.0007	0.5774	0.0163	0.0736	0.0018	0.8647	458	11
GE15-22	0.24	489	0.0569	0.0007	0.6357	0.0170	0.0810	0.0020	0.9015	502	12
GE15-23	0.15	764	0.0532	0.0006	0.4004	0.0104	0.0546	0.0013	0.9386	343	8
GE15-24	0.04	818	0.0556	0.0006	0.5675	0.0144	0.0740	0.0018	0.9510	460	11
GE15-25	0.10	779	0.0587	0.0007	0.6390	0.0167	0.0790	0.0019	0.9385	490	12
GE15-26	0.10	691	0.0588	0.0008	0.7760	0.0244	0.0957	0.0023	0.7612	589	13
GE15-27	0.29	548	0.0562	0.0007	0.5653	0.0155	0.0729	0.0018	0.9125	454	11
GE15-30	0.20	167	0.0562	0.0007	0.5691	0.0167	0.0735	0.0018	0.8473	457	11
GE15-32	0.42	4353	0.0567	0.0006	0.5450	0.0141	0.0697	0.0017	0.9416	434	10
GE15-33	0.41	1289	0.0542	0.0006	0.4604	0.0122	0.0616	0.0015	0.9221	385	9
GE15-34	0.23	320	0.0559	0.0007	0.5474	0.0149	0.0710	0.0018	0.9084	442	11
GE15-35	0.29	1993	0.0624	0.0007	0.7765	0.0196	0.0903	0.0022	0.9681	557	13
GE15-36	0.27	1131	0.0581	0.0007	0.5971	0.0153	0.0746	0.0018	0.9554	464	11
GE15-37	0.16	231	0.0580	0.0007	0.5918	0.0166	0.0740	0.0018	0.8855	460	11
GE15-38	0.10	1256	0.0583	0.0007	0.4504	0.0118	0.0560	0.0014	0.9376	351	8
GE15-39	0.51	296	0.0578	0.0007	0.5513	0.0155	0.0691	0.0017	0.8724	431	10

GE17											
Spot	**Th/U**	**U ppm**	**^{207}Pb/ ^{206}Pb**	**1σ**	**^{207}Pb/ ^{235}U**	**1σ**	**^{206}Pb/ ^{238}U**	**1σ**	**error corr**	**^{206}Pb/^{238}U age (Ma)**	**1σ**
GE17-1	0.41	309	0.0525	0.0007	0.3529	0.0100	0.0487	0.0012	0.8728	307	7
GE17-2	0.33	369	0.0567	0.0007	0.5461	0.0159	0.0699	0.0018	0.8851	435	11
GE17-3	0.53	602	0.0560	0.0007	0.5407	0.0143	0.0700	0.0017	0.9292	436	10
GE17-4	0.17	450	0.0560	0.0007	0.5029	0.0136	0.0651	0.0016	0.9103	407	10
GE17-5	0.55	293	0.0558	0.0007	0.5351	0.0149	0.0695	0.0017	0.8744	433	10
GE17-6	0.93	137	0.0522	0.0008	0.3396	0.0113	0.0472	0.0012	0.7526	297	7
GE17-7	0.47	134	0.0545	0.0008	0.3643	0.0120	0.0485	0.0012	0.7656	305	8
GE17-8	0.20	278	0.0581	0.0007	0.6087	0.0170	0.0759	0.0019	0.8849	472	11
GE17-9	0.01	1079	0.0535	0.0007	0.3651	0.0116	0.0495	0.0013	0.8302	311	8
GE17-10	0.14	525	0.0543	0.0007	0.4193	0.0129	0.0561	0.0015	0.8537	352	9
GE17-11	0.73	101	0.0530	0.0010	0.3360	0.0124	0.0460	0.0012	0.6842	290	7
GE17-14	0.41	168	0.0536	0.0007	0.3572	0.0110	0.0483	0.0012	0.8116	304	7
GE17-15	0.26	1595	0.0529	0.0006	0.3942	0.0102	0.0541	0.0013	0.9471	339	8
GE17-16	0.33	218	0.0532	0.0007	0.3986	0.0117	0.0544	0.0014	0.8517	341	8
GE17-17	0.31	231	0.0539	0.0007	0.3555	0.0105	0.0478	0.0012	0.8473	301	7
GE17-18	0.19	579	0.0562	0.0007	0.4638	0.0125	0.0599	0.0015	0.9207	375	9
GE17-20	0.26	172	0.0520	0.0007	0.3774	0.0118	0.0526	0.0013	0.8079	331	8
GE17-21	0.07	483	0.0554	0.0008	0.5037	0.0175	0.0660	0.0017	0.7467	412	10
GE17-23	0.13	389	0.0563	0.0007	0.5511	0.0150	0.0711	0.0018	0.9138	443	11
GE17-24	0.22	1182	0.0542	0.0006	0.4260	0.0112	0.0570	0.0014	0.9509	357	9

Table S1 (continued): LA–ICP–MS zircon U–Pb isotopic analytical data of sample N1–N4 and GE15, GE17, GE18. The letter "a" with the number of sample indicates that these age figures are obtained from the core of zircon crystals and the remaining figures are from the rim of crystals.

GE17												
Spot	Th/U	U ppm	^{207}Pb/ ^{206}Pb	1σ	^{207}Pb/ ^{235}U	1σ	^{206}Pb/ ^{238}U	1σ	error corr	^{206}Pb/^{238}U age (Ma)	1σ
GE17-26	0.20	829	0.0544	0.0006	0.3597	0.0095	0.0480	0.0012	0.9299	302	7
GE17-27	0.17	443	0.0528	0.0006	0.3545	0.0099	0.0487	0.0012	0.8980	307	7
GE17-28	0.28	437	0.0578	0.0007	0.5153	0.0139	0.0647	0.0016	0.9037	404	10
GE17-29	0.67	162	0.0552	0.0009	0.3728	0.0130	0.0490	0.0013	0.7640	308	8
GE17-30	0.26	233	0.0566	0.0007	0.5633	0.0161	0.0722	0.0018	0.8796	449	11
GE17-31	0.21	1341	0.0539	0.0012	0.4649	0.0190	0.0625	0.0016	0.6093	391	9
GE17-32	0.13	414	0.0574	0.0007	0.6015	0.0163	0.0760	0.0019	0.9117	472	11
GE17-33	0.31	121	0.0513	0.0008	0.3482	0.0116	0.0492	0.0013	0.7677	310	8

GE18												
Spot	Th/U	U ppm	^{207}Pb/ ^{206}Pb	1σ	^{207}Pb/ ^{235}U	1σ	^{206}Pb/ ^{238}U	1σ	error corr	^{206}Pb/^{238}U age (Ma)	1σ
GE18-1	0.48	632	0.0542	0.0006	0.3589	0.0091	0.0481	0.0012	0.9702	303	7
GE18-3	0.30	371	0.0544	0.0006	0.3876	0.0100	0.0517	0.0013	0.9567	325	8
GE18-4	0.20	686	0.0522	0.0006	0.3783	0.0096	0.0525	0.0013	0.9687	330	8
GE18-5	0.65	529	0.0524	0.0006	0.3682	0.0094	0.0510	0.0013	0.9572	321	8
GE18-6	0.36	239	0.0546	0.0006	0.3939	0.0104	0.0523	0.0013	0.9280	329	8
GE18-7	0.40	206	0.0531	0.0006	0.3770	0.0101	0.0515	0.0013	0.9163	324	8
GE18-8	0.20	396	0.0528	0.0006	0.4005	0.0104	0.0550	0.0013	0.9379	345	8
GE18-9	0.23	445	0.0527	0.0006	0.3772	0.0098	0.0519	0.0013	0.9395	326	8
GE18-10	0.16	84	0.0559	0.0007	0.5597	0.0157	0.0726	0.0018	0.8746	452	11
GE18-11	0.25	385	0.0537	0.0006	0.3971	0.0105	0.0536	0.0013	0.9263	337	8
GE18-12	0.25	2386	0.0532	0.0006	0.3771	0.0095	0.0514	0.0013	0.9707	323	8
GE18-13	0.76	4617	0.0534	0.0006	0.3672	0.0093	0.0499	0.0012	0.9712	314	7
GE18-14	0.42	1527	0.0523	0.0006	0.3782	0.0096	0.0525	0.0013	0.9531	330	8
GE18-16	0.37	934	0.0530	0.0006	0.3818	0.0100	0.0523	0.0013	0.9345	329	8
GE18-17	0.36	2461	0.0535	0.0006	0.3738	0.0099	0.0507	0.0013	0.9438	319	8
GE18-18	0.26	383	0.0531	0.0006	0.3850	0.0107	0.0526	0.0013	0.8860	331	8
GE18-19	0.27	534	0.0530	0.0006	0.3803	0.0104	0.0521	0.0013	0.9041	327	8
GE18-21	0.25	1299	0.0532	0.0006	0.3769	0.0101	0.0514	0.0013	0.9262	323	8
GE18-22	0.43	468	0.0520	0.0006	0.3614	0.0102	0.0504	0.0013	0.8782	317	8
GE18-23	0.29	4191	0.0530	0.0006	0.3701	0.0094	0.0507	0.0012	0.9686	319	8
GE18-24	0.41	788	0.0555	0.0006	0.3839	0.0101	0.0502	0.0012	0.9386	316	8
GE18-25	0.22	424	0.0529	0.0006	0.3855	0.0105	0.0529	0.0013	0.9073	332	8
GE18-27	0.19	2732	0.0530	0.0006	0.3817	0.0098	0.0523	0.0013	0.9613	328	8
GE18-28	0.22	657	0.0525	0.0013	0.3636	0.0161	0.0502	0.0013	0.5836	316	8
GE18-29	0.49	532	0.0524	0.0006	0.3664	0.0100	0.0508	0.0013	0.9061	319	8
GE18-30	0.48	1632	0.0529	0.0006	0.3943	0.0103	0.0541	0.0013	0.9392	339	8
GE18-32	0.26	2317	0.0557	0.0006	0.4019	0.0106	0.0523	0.0013	0.9442	329	8
GE18-33	0.27	1028	0.0537	0.0006	0.3916	0.0106	0.0529	0.0013	0.9172	332	8

Table S2: LA–ICP–MS zircon U–Pb isotopic analytical data of sample 1Z, 2Z, 3Z, 4Z, 5Z, 7Z and GE30.

					1Z						
Spot	Th/U	U ppm	^{207}Pb/ ^{206}Pb	1σ	^{207}Pb/ ^{235}U	1σ	^{206}Pb/ ^{238}U	1σ	error corr	^{206}Pb/^{238}U age (Ma)	1σ
1Z-1	0.40	300	0.05593	0.00068	0.57768	0.01604	0.07492	0.00181	0.02315	466	11
1Z-2	0.41	508	0.05561	0.00065	0.56483	0.01515	0.07367	0.00179	0.02485	458	11
1Z-3	0.23	1245	0.05554	0.00063	0.47907	0.01243	0.06256	0.00151	0.02201	391	9
1Z-4	0.03	618	0.05271	0.00063	0.37535	0.01026	0.05165	0.00125	0.02404	325	8
1Z-5	0.50	851	0.05618	0.00065	0.53301	0.01421	0.06881	0.00166	0.02357	429	10
1Z-6	0.57	828	0.05573	0.00067	0.53459	0.01469	0.06958	0.00163	0.02282	434	10
1Z-7	0.29	198	0.05445	0.00068	0.56339	0.01609	0.07505	0.00184	0.02304	467	11
1Z-8	0.43	206	0.06784	0.00078	1.25273	0.03291	0.13395	0.00316	0.04221	810	18
1Z-9	0.60	1251	0.0634	0.00069	0.91849	0.02276	0.10508	0.00251	0.03434	644	15
1Z-10	0.51	459	0.05599	0.00064	0.60159	0.01581	0.07793	0.00187	0.0248	484	11
1Z-11	0.46	560	0.05677	0.00065	0.57242	0.01494	0.07314	0.00175	0.02328	455	11
1Z-12	0.42	382	0.05696	0.00067	0.60809	0.0163	0.07743	0.00187	0.02336	481	11
1Z-13	0.01	571	0.05083	0.0006	0.35238	0.0096	0.05028	0.00122	0.01865	316	7
1Z-14	0.33	544	0.05788	0.00067	0.59037	0.0157	0.07398	0.00178	0.02391	460	11
1Z-15	0.46	619	0.05635	0.00065	0.57511	0.01531	0.07402	0.00178	0.02319	460	11
1Z-16	0.60	478	0.05606	0.00068	0.59384	0.01661	0.07683	0.00188	0.02381	477	11
1Z-17	0.43	327	0.05684	0.00071	0.60214	0.01717	0.07683	0.00186	0.02424	477	11
1Z-18	0.70	293	0.06754	0.00077	1.24018	0.03247	0.13321	0.00322	0.04263	806	18
1Z-19	0.26	139	0.06499	0.0008	1.10228	0.03093	0.12305	0.00299	0.03867	748	17
1Z-20	0.44	547	0.05721	0.00066	0.58906	0.01555	0.0747	0.0018	0.0237	464	11
1Z-21	0.37	237	0.05918	0.00073	0.65679	0.01844	0.08052	0.00195	0.02643	499	12
1Z-22	0.36	471	0.05668	0.00066	0.58233	0.01558	0.07453	0.00179	0.02534	463	11
1Z-23	0.44	471	0.05689	0.00066	0.60072	0.01608	0.0766	0.00183	0.02467	476	11
1Z-24	0.23	634	0.05504	0.00064	0.47724	0.01281	0.06289	0.00151	0.02636	393	9
1Z-25	0.56	450	0.05674	0.00067	0.57833	0.0157	0.07393	0.00177	0.02387	460	11
1Z-26	0.33	133	0.06218	0.00101	0.64425	0.02262	0.07516	0.00195	0.02811	467	12
1Z-27	0.09	993	0.05372	0.00063	0.4099	0.01101	0.05535	0.00133	0.02744	347	8
1Z-28	0.47	861	0.05842	0.00064	0.71833	0.01809	0.08918	0.0021	0.02404	551	12
1Z-29	0.31	718	0.05598	0.00064	0.56647	0.01472	0.07339	0.00178	0.0208	457	11
1Z-30	0.50	342	0.05685	0.00068	0.60358	0.01655	0.07701	0.00187	0.02287	478	11
1Z-31	0.39	427	0.05689	0.00067	0.60937	0.01657	0.0777	0.00189	0.02342	482	11
1Z-32	1.08	494	0.06095	0.00071	0.78859	0.02114	0.09384	0.00229	0.02904	578	13
1Z-33	0.26	235	0.06004	0.00108	0.68599	0.02625	0.08288	0.0023	0.02996	513	14

					2Z						
Spot	Th/U	U ppm	^{207}Pb/ ^{206}Pb	1σ	^{207}Pb/ ^{235}U	1σ	^{206}Pb/ ^{238}U	1σ	error corr	^{206}Pb/^{238}U age (Ma)	1σ
2Z-1	0.32	264	0.05658	0.00069	0.59777	0.01676	0.07662	0.00186	0.02348	476	11
2Z-2	0.13	2304	0.05602	0.00062	0.57067	0.01437	0.07388	0.00176	0.02356	459	11
2Z-3	0.30	616	0.05681	0.00065	0.57948	0.01519	0.07399	0.00175	0.02303	460	11
2Z-4	0.13	801	0.05381	0.00062	0.41411	0.01097	0.05582	0.00134	0.02478	350	8
2Z-5	0.41	1067	0.05645	0.00064	0.59798	0.01545	0.07684	0.00182	0.02303	477	11
2Z-6	0.55	341	0.0576	0.00072	0.58026	0.01647	0.07306	0.00174	0.02439	455	10
2Z-7	0.46	120	0.05582	0.00086	0.58297	0.01946	0.07576	0.00191	0.02376	471	11
2Z-8	0.33	818	0.05547	0.00065	0.51761	0.01385	0.06769	0.00163	0.02368	422	10
2Z-9	0.61	167	0.05748	0.0008	0.58233	0.018	0.07349	0.00178	0.02286	457	11
2Z-10	0.30	671	0.0552	0.00072	0.45367	0.01342	0.05961	0.00148	0.02018	373	9
2Z-11	0.47	516	0.05738	0.00065	0.58799	0.01521	0.07432	0.00177	0.02303	462	11
2Z-12	0.42	202	0.05827	0.00073	0.60983	0.01735	0.07591	0.00183	0.02416	472	11
2Z-13	1.06	309	0.05953	0.00069	0.71946	0.01924	0.08766	0.00211	0.02824	542	13
2Z-14	0.62	943	0.05794	0.00065	0.5876	0.01498	0.07356	0.00176	0.02314	458	11
2Z-15	0.41	471	0.05626	0.00065	0.53899	0.01439	0.06949	0.00167	0.02316	433	10
2Z-16	0.53	753	0.05682	0.00064	0.607	0.01575	0.07749	0.00185	0.02422	481	11
2Z-17	0.52	544	0.05798	0.00067	0.58257	0.01551	0.07288	0.00174	0.02386	453	10

Table S2 (continued): LA–ICP–MS zircon U–Pb isotopic analytical data of sample 1Z, 2Z, 3Z, 4Z, 5Z, 7Z and GE30.

2Z											
Spot	Th/U	U ppm	$^{207}Pb/\,^{206}Pb$	1σ	$^{207}Pb/\,^{235}U$	1σ	$^{206}Pb/\,^{238}U$	1σ	error corr	$^{206}Pb/^{238}U$ age (Ma)	1σ
2Z-18	0.59	511	0.05744	0.00067	0.62563	0.01675	0.079	0.0019	0.02973	490	11
2Z-19	0.44	249	0.12381	0.0014	5.10383	0.13207	0.29901	0.00716	0.06794	1686	36
2Z-20	0.77	76	0.06434	0.00095	0.93843	0.0304	0.1058	0.00263	0.03287	648	15
2Z-21	0.51	352	0.05635	0.0007	0.57737	0.01635	0.07432	0.0018	0.02442	462	11
Z2-22	0.57	210	0.05785	0.00073	0.59328	0.01696	0.07438	0.00179	0.02337	462	11
Z2-23	0.42	254	0.0568	0.0007	0.55306	0.01548	0.07062	0.00171	0.02428	440	10
Z2-24	0.64	979	0.05727	0.00064	0.57376	0.01465	0.07266	0.00174	0.02282	452	10
Z2-25	0.47	912	0.09443	0.02081	0.68651	0.17519	0.05273	0.00229	0.01549	331	14
Z2-26	0.47	161	0.06495	0.00086	0.95471	0.02813	0.10662	0.00251	0.03388	653	15

3Z											
Spot	Th/U	U ppm	$^{207}Pb/\,^{206}Pb$	1σ	$^{207}Pb/\,^{235}U$	1σ	$^{206}Pb/\,^{238}U$	1σ	error corr	$^{206}Pb/^{238}U$ age (Ma)	1σ
3Z-1	0.23	478	0.05284	0.00063	0.38212	0.01051	0.05245	0.00129	0.0164	330	8
3Z-2	0.61	383	0.0597	0.00069	0.86587	0.02286	0.1052	0.00258	0.03239	645	15
3Z-3	0.27	455	0.06036	0.00069	0.86474	0.02266	0.10391	0.00254	0.03256	637	15
3Z-4	0.48	341	0.07098	0.00081	1.60113	0.0416	0.1636	0.00401	0.05226	977	22
3Z-5	0.37	176	0.06273	0.00077	0.92151	0.02602	0.10654	0.00265	0.03437	653	15
3Z-6	1.22	93	0.05765	0.00085	0.73555	0.02398	0.09255	0.00234	0.02843	571	14
3Z-7	0.49	325	0.05297	0.00068	0.37779	0.01112	0.05173	0.0013	0.01585	325	8
3Z-8	0.40	464	0.05835	0.00069	0.76533	0.02073	0.09514	0.00235	0.02901	586	14
3Z-9	0.48	351	0.05718	0.0007	0.61164	0.01724	0.07758	0.00193	0.02389	482	12
3Z-10	0.99	377	0.06004	0.00072	0.8686	0.02399	0.10493	0.00261	0.03221	643	15
3Z-11	0.33	224	0.05997	0.00077	0.77106	0.0225	0.09326	0.00235	0.02833	575	14
3Z-12	0.71	1382	0.0688	0.00076	1.22094	0.03055	0.12872	0.00311	0.03705	781	18
3Z-13	0.10	418	0.06121	0.0007	0.86051	0.02256	0.10196	0.00248	0.02914	626	15
3Z-14	0.32	661	0.05823	0.00068	0.58656	0.01564	0.07307	0.00178	0.02192	455	11
3Z-15	0.37	386	0.17083	0.0019	9.05936	0.22844	0.38464	0.00933	0.1099	2098	43
3Z-16	0.93	214	0.12994	0.00146	6.45683	0.16531	0.36039	0.00873	0.09911	1984	41
3Z-17	0.32	169	0.17897	0.00202	11.92533	0.3062	0.48326	0.01177	0.12766	2541	51
3Z-18	0.73	87	0.06613	0.00094	0.93827	0.0298	0.1029	0.0026	0.03024	631	15
3Z-19	0.56	60	0.06268	0.00114	0.85085	0.03223	0.09846	0.00262	0.02892	605	15
3Z-20	0.18	607	0.0608	0.00072	0.76173	0.02066	0.09087	0.00224	0.02989	561	13
3Z-21	1.01	171	0.07418	0.00091	1.68069	0.04722	0.16433	0.00407	0.04745	981	23
3Z-22	0.46	278	0.29189	0.00349	23.6654	0.66248	0.58803	0.01388	0.15484	2981	56
3Z-23	0.98	81	0.14131	0.00161	7.57969	0.19748	0.38906	0.0096	0.11113	2118	45
3Z-24	0.81	429	0.05864	0.00069	0.64048	0.01732	0.07923	0.00193	0.02648	492	12
3Z-25	0.60	174	0.05818	0.00075	0.75486	0.02215	0.0941	0.00234	0.02926	580	14
3Z-26	0.29	219	0.06152	0.00075	0.92669	0.02592	0.10925	0.00271	0.03431	668	16
3Z-27	0.37	117	0.06404	0.00085	1.0101	0.03033	0.11441	0.00283	0.03695	698	16

4Z											
Spot	Th/U	U ppm	$^{207}Pb/\,^{206}Pb$	1σ	$^{207}Pb/\,^{235}U$	1σ	$^{206}Pb/\,^{238}U$	1σ	error corr	$^{206}Pb/^{238}U$ age (Ma)	1σ
4Z-1	0.31	1157	0.05603	0.00064	0.60215	0.01587	0.07796	0.0019	0.924718475	484	11
4Z-2	0.36	855	0.05622	0.00067	0.5508	0.01512	0.07107	0.00175	0.897002955	443	11
4Z-3	0.32	1187	0.0552	0.00186	0.55022	0.02781	0.0723	0.00183	0.500781384	450	11
4Z-4	0.17	397	0.05626	0.00071	0.47991	0.01386	0.06188	0.00152	0.850530422	387	9
4Z-5	0.67	386	0.05455	0.00069	0.58941	0.01694	0.07838	0.00191	0.847875726	486	11
4Z-6	0.22	963	0.0546	0.00062	0.46521	0.01214	0.0618	0.00151	0.9363082	387	9
4Z-7	0.26	492	0.0537	0.00063	0.54685	0.01476	0.07386	0.00181	0.907927416	459	11
4Z-8	0.41	734	0.05559	0.00064	0.53312	0.01399	0.06957	0.00169	0.92570362	434	10
4Z-9	0.29	290	0.05582	0.00069	0.51561	0.01463	0.067	0.00166	0.873193091	418	10
4Z-10	0.56	303	0.06021	0.00075	0.62652	0.01796	0.07548	0.00187	0.864247878	469	11
4Z-11	0.14	1003	0.05561	0.00064	0.50228	0.01324	0.06552	0.0016	0.926411621	409	10

Table S2 (continued): LA–ICP–MS zircon U–Pb isotopic analytical data of sample 1Z, 2Z, 3Z, 4Z, 5Z, 7Z and GE30.

4Z											
Spot	Th/U	U ppm	$^{207}Pb/^{206}Pb$	1σ	$^{207}Pb/^{235}U$	1σ	$^{206}Pb/^{238}U$	1σ	error corr	$^{206}Pb/^{238}U$ age (Ma)	1σ
4Z-12	0.55	709	0.05731	0.00067	0.60086	0.01603	0.07605	0.00186	0.916755443	473	11
4Z-13	0.43	481	0.05619	0.00067	0.58897	0.01615	0.07603	0.00187	0.896968648	472	11
4Z-14	0.60	206	0.05598	0.00076	0.59452	0.01825	0.07704	0.00194	0.820330872	478	12
4Z-15	0.40	720	0.05664	0.00067	0.59047	0.01608	0.07562	0.00185	0.89835264	470	11
4Z-16	0.06	945	0.05375	0.00065	0.38801	0.01073	0.05236	0.00128	0.884002572	329	8
4Z-17	0.33	1515	0.0568	0.00063	0.5807	0.01473	0.07415	0.00181	0.962313323	461	11
4Z-18	0.65	259	0.0568	0.0007	0.59094	0.0166	0.07546	0.00185	0.872750743	469	11
4Z-19	0.21	1297	0.0549	0.00062	0.50138	0.01291	0.06625	0.00162	0.949663826	414	10
4Z-20	0.33	291	0.05755	0.00071	0.55036	0.0155	0.06936	0.00172	0.880510474	432	10
4Z-21	0.19	950	0.05396	0.00062	0.45173	0.01191	0.06072	0.00149	0.930725639	380	9
4Z-22	0.20	1546	0.0551	0.00064	0.47345	0.01249	0.06232	0.00154	0.936709573	390	9
4Z-23	0.49	1078	0.05572	0.00064	0.57202	0.01502	0.07446	0.00183	0.93598597	463	11
4Z-24	0.45	532	0.05655	0.00067	0.59468	0.01616	0.07627	0.00187	0.90225612	474	11
4Z-25	0.01	2399	0.05294	0.00063	0.38676	0.01056	0.05299	0.00133	0.919253633	333	8
4Z-26	0.27	1175	0.05656	0.00066	0.59763	0.01596	0.07664	0.00187	0.913662107	476	11
4Z-27	0.07	808	0.05551	0.00067	0.41535	0.01147	0.05427	0.00134	0.894119926	341	8
4Z-28	0.31	278	0.05803	0.00088	0.52816	0.0178	0.06602	0.00177	0.795505618	412	11
4Z-29	0.52	249	0.05693	0.0007	0.6015	0.01702	0.07664	0.00188	0.866918816	476	11
4Z-30	0.46	448	0.05666	0.00067	0.61233	0.01668	0.07839	0.00194	0.908511767	487	12
4Z-31	0.44	562	0.05732	0.00066	0.60119	0.01594	0.07607	0.00186	0.922195416	473	11
4Z-32	0.26	588	0.05556	0.00065	0.51704	0.01385	0.0675	0.00165	0.912545527	421	10
4Z-33	0.23	391	0.05733	0.00076	0.59886	0.01821	0.07576	0.00196	0.850807805	471	12
4Z-34	0.25	513	0.05612	0.00067	0.49033	0.01342	0.06337	0.00154	0.887918211	396	9
4Z-35	0.41	553	0.05691	0.00068	0.6171	0.01686	0.07865	0.00192	0.893512182	488	11
4Z-36	0.40	1346	0.0565	0.00065	0.60154	0.01581	0.07723	0.00188	0.926199316	480	11
4Z-37	0.65	500	0.05697	0.00068	0.60476	0.01661	0.07699	0.00189	0.893801153	478	11
4Z-38	0.22	708	0.05548	0.00067	0.49217	0.01356	0.06434	0.00156	0.880033065	402	9
4Z-39	0.03	1934	0.05276	0.00062	0.37803	0.01021	0.05197	0.00126	0.897673392	327	8

| 5Z											
Spot	Th/U	U ppm	$^{207}Pb/^{206}Pb$	1σ	$^{207}Pb/^{235}U$	1σ	$^{206}Pb/^{238}U$	1σ	error corr	$^{206}Pb/^{238}U$ age (Ma)	1σ
5Z-1	0.01	5017	0.05309	0.00059	0.39874	0.01011	0.05448	0.0013	0.941119782	342	8
5Z-2	0.00	2603	0.05391	0.00059	0.40628	0.01007	0.05466	0.0013	0.959554614	343	8
5Z-3	0.01	4963	0.05315	0.00061	0.41633	0.01095	0.05682	0.0014	0.936807575	356	9
5Z-4	0.01	7962	0.05278	0.00059	0.40883	0.01047	0.05618	0.00138	0.959165229	352	8
5Z-5	0.06	3051	0.0536	0.00058	0.47072	0.01164	0.0637	0.00148	0.939576084	398	9
5Z-6	0.02	4910	0.0528	0.00063	0.398	0.0096	0.05467	0.00115	0.872088592	343	7
5Z-7	0.04	1072	0.05355	0.00061	0.40321	0.01049	0.05462	0.00131	0.92188215	343	8
5Z-8	0.32	384	0.05571	0.00098	0.55603	0.02069	0.07239	0.00194	0.720212885	451	12
5Z-9	1.20	637	0.0603	0.00069	0.83057	0.02172	0.09991	0.0024	0.918583631	614	14
5Z-10	0.08	3668	0.05373	0.0006	0.44452	0.01136	0.06	0.00142	0.926083333	376	9
5Z-11	0.86	972	0.06131	0.0007	0.82967	0.02179	0.09815	0.00237	0.919403597	604	14
5Z-12	0.49	137	0.10952	0.00243	4.57679	0.17404	0.30308	0.00673	0.583941978	1707	33
5Z-13	0.13	3881	0.05359	0.00123	0.46415	0.01689	0.06282	0.00133	0.581811651	393	8
5Z-14	0.28	353	0.06799	0.00161	1.32613	0.05267	0.14147	0.00324	0.576638238	853	18
5Z-15	1.05	199	0.06854	0.00079	1.33884	0.03537	0.14168	0.00339	0.905700837	854	19
5Z-16	0.22	1127	0.05564	0.00062	0.54865	0.01397	0.07153	0.00171	0.938873028	445	10
5Z-17	0.33	953	0.05537	0.00062	0.48542	0.01255	0.06359	0.00152	0.924546381	397	9
5Z-18	0.03	1873	0.05289	0.00059	0.42111	0.01076	0.05775	0.00137	0.928435765	362	8
5Z-19	1.01	170	0.17087	0.00191	9.47193	0.24097	0.40207	0.00968	0.946344341	2179	45
5Z-20	0.07	1004	0.05468	0.00063	0.47759	0.01254	0.06335	0.00152	0.913807371	396	9
5Z-21	0.08	2094	0.05395	0.00061	0.41001	0.01063	0.05512	0.0013	0.909693995	346	8
5Z-22	0.24	448	0.05296	0.00065	0.40065	0.01121	0.05487	0.00133	0.86631576	344	8
5Z-23	0.12	320	0.05649	0.00081	0.46158	0.01489	0.05927	0.00154	0.805449059	371	9
5Z-24	0.02	4124	0.05382	0.00067	0.44336	0.01073	0.05974	0.00123	0.850739661	374	7
5Z-25	0.45	560	0.05908	0.00067	0.66369	0.01728	0.08148	0.00195	0.919189653	505	12

Table S2 (continued): LA-ICP-MS zircon U-Pb isotopic analytical data of sample 1Z, 2Z, 3Z, 4Z, 5Z, 7Z and GE30.

						5Z					
Spot	Th/U	U ppm	$^{207}Pb/^{206}Pb$	1σ	$^{207}Pb/^{235}U$	1σ	$^{206}Pb/^{238}U$	1σ	error corr	$^{206}Pb/^{238}U$ age (Ma)	1σ
5Z-26	0.00	2753	0.05321	0.00058	0.3797	0.00948	0.05175	0.00122	0.94423857	325	7
5Z-27	0.47	399	0.06065	0.00069	0.81638	0.02131	0.09763	0.00234	0.918208852	601	14
5Z-28	0.10	1845	0.05802	0.00066	0.50125	0.01311	0.06266	0.00152	0.927480722	392	9
5Z-29	0.06	745	0.05701	0.00065	0.57181	0.01491	0.07275	0.00174	0.917255561	453	10
5Z-30	0.35	324	0.05658	0.00074	0.54429	0.01618	0.06978	0.00174	0.838822597	435	10
5Z-31	0.01	8549	0.05364	0.0006	0.40448	0.00921	0.05469	0.00113	0.907419154	343	7
5Z-32	0.01	6398	0.05634	0.00064	0.46503	0.01083	0.05986	0.00125	0.896655909	375	8
5Z-33	0.02	4555	0.05416	0.00078	0.38505	0.01028	0.05156	0.00107	0.777311123	324	7
5Z-34	0.62	89	0.07107	0.00094	1.43467	0.04303	0.14643	0.00368	0.837912033	881	21
5Z-35	0.06	3649	0.05617	0.0006	0.46217	0.01131	0.05968	0.00139	0.951754924	374	8
5Z-36	0.32	1170	0.05793	0.00065	0.57727	0.01472	0.07228	0.00173	0.938640173	450	10
5Z-37	0.00	7433	0.05303	0.00059	0.416	0.01052	0.0569	0.00137	0.952107292	357	8
5Z-38	0.01	2604	0.0535	0.00058	0.40937	0.01017	0.0555	0.0013	0.94285613	348	8
5Z-39	0.37	598	0.06055	0.00067	0.85613	0.02176	0.10256	0.00242	0.928363759	629	14
5Z-40	0.07	1217	0.05437	0.00061	0.4418	0.01125	0.05894	0.0014	0.93280549	369	9
5Z-41	0.06	3855	0.05257	0.00058	0.41644	0.01043	0.05746	0.00136	0.945020906	360	8
5Z-42	0.28	511	0.16005	0.00176	9.12842	0.22902	0.41369	0.00982	0.946147113	2232	45
5Z-43	1.00	693	0.06037	0.00069	0.66609	0.01737	0.08002	0.0019	0.910517189	496	11
5Z-44	0.03	5921	0.05227	0.00058	0.42437	0.01079	0.05889	0.00139	0.928317368	369	8
5Z-45	0.45	936	0.0648	0.00069	1.07554	0.02596	0.12038	0.00284	0.977430484	733	16
5Z-46	0.01	5190	0.05191	0.00055	0.41937	0.01005	0.0586	0.00138	0.982681473	367	8
5Z-47	0.03	1175	0.05144	0.00059	0.36963	0.00965	0.05211	0.00127	0.933517678	327	8

						7Z					
Spot	Th/U	U ppm	$^{207}Pb/^{206}Pb$	1σ	$^{207}Pb/^{235}U$	1σ	$^{206}Pb/^{238}U$	1σ	error corr	$^{206}Pb/^{238}U$ age (Ma)	1σ
7Z-1	0.48	109	0.06122	0.00078	0.84168	0.02432	0.09971	0.00242	0.839962866	613	14
7Z-2	0.08	774	0.05428	0.00072	0.38504	0.01166	0.05145	0.00133	0.853637647	323	8
7Z-3	0.69	72	0.05179	0.0011	0.34365	0.01413	0.04813	0.00123	0.621531918	303	8
7Z-4	0.14	3510	0.05984	0.00065	0.42518	0.01054	0.05153	0.00122	0.955062746	324	7
7Z-5	0.06	320	0.05857	0.00072	0.69023	0.01932	0.08548	0.0021	0.877690688	529	12
7Z-6	0.36	333	0.05551	0.00066	0.58087	0.01576	0.0759	0.00182	0.88379664	472	11
7Z-7	0.52	191	0.05232	0.00074	0.35324	0.01101	0.04897	0.00119	0.779649518	308	7
7Z-8	0.56	1017	0.05792	0.00063	0.58101	0.0144	0.07276	0.00171	0.948253676	453	10
7Z-9	0.33	109	0.05285	0.00097	0.39445	0.01489	0.05413	0.00139	0.680258592	340	9
7Z-10	0.35	258	0.05566	0.00068	0.54463	0.0152	0.07097	0.00168	0.848188634	442	10
7Z-11	0.31	601	0.05653	0.00067	0.56042	0.0152	0.07192	0.00169	0.866377298	448	10
7Z-12	0.25	1390	0.05569	0.00061	0.43434	0.01094	0.05657	0.00131	0.919385441	355	8
7Z-13	0.39	252	0.05268	0.00069	0.36596	0.0108	0.05038	0.00122	0.820562245	317	7
7Z-14	1.18	272	0.05343	0.0008	0.34764	0.01146	0.0472	0.00119	0.764803887	297	7
7Z-15	0.06	821	0.05508	0.00062	0.50498	0.01311	0.0665	0.00156	0.90359629	415	9
7Z-16	0.41	336	0.05315	0.00072	0.35986	0.01086	0.04911	0.00116	0.782693641	309	7
7Z-17	0.76	857	0.05672	0.00065	0.55292	0.01448	0.0707	0.00168	0.907368306	440	10
7Z-18	0.22	575	0.05367	0.00064	0.40467	0.0111	0.05469	0.00131	0.873255647	343	8
7Z-19	0.07	1921	0.05578	0.00061	0.38456	0.00954	0.05001	0.00116	0.935011321	315	7
7Z-20	0.18	526	0.05555	0.00064	0.44943	0.01188	0.05869	0.00138	0.889529991	368	8
7Z-21	0.46	1111	0.05638	0.00063	0.55056	0.01397	0.07083	0.00169	0.940324414	441	10
7Z-22	0.22	457	0.05177	0.00063	0.35834	0.0099	0.0502	0.00119	0.858031712	316	7
7Z-23	0.24	747	0.05231	0.00061	0.36675	0.00976	0.05085	0.00122	0.901548673	320	7
7Z-24	0.53	516	0.05356	0.00065	0.36998	0.0102	0.05011	0.0012	0.86863019	315	7
7Z-25	0.32	626	0.05881	0.00068	0.65147	0.01717	0.08034	0.00193	0.911485172	498	12
7Z-26	0.24	499	0.05441	0.00067	0.3612	0.0101	0.04815	0.00115	0.85413775	303	7
7Z-27	0.93	321	0.05551	0.00084	0.36528	0.01215	0.04773	0.00122	0.768454242	301	8
7Z-28	0.08	814	0.05447	0.00064	0.41539	0.01126	0.05531	0.00133	0.887085804	347	8
7Z-29	1.35	124	0.05288	0.00637	0.35826	0.05183	0.04913	0.0015	0.211038459	309	9
7Z-30	0.18	433	0.05631	0.00065	0.5869	0.01565	0.0756	0.00181	0.897855706	470	11

Table S2 (continued): LA–ICP–MS zircon U–Pb isotopic analytical data of sample 1Z, 2Z, 3Z, 4Z, 5Z, 7Z and GE30.

GE30											
Spot	Th/U	U ppm	$^{207}Pb/^{206}Pb$	1σ	$^{207}Pb/^{235}U$	1σ	$^{206}Pb/^{238}U$	1σ	error corr	$^{206}Pb/^{238}U$ age (Ma)	1σ
GE30-1	0.15	345	0.0574	0.0006	0.6005	0.0153	0.0759	0.0018	0.9244	472	11
GE30-2	0.16	286	0.0574	0.0007	0.6225	0.0171	0.0786	0.0019	0.8868	488	11
GE30-3	0.21	536	0.0558	0.0006	0.5357	0.0137	0.0696	0.0017	0.9280	434	10
GE30-5	0.26	399	0.0574	0.0006	0.5912	0.0152	0.0748	0.0018	0.9256	465	11
GE30-8	0.56	215	0.0592	0.0007	0.7401	0.0202	0.0906	0.0022	0.8908	559	13
GE30-9	0.19	1307	0.0564	0.0006	0.6166	0.0156	0.0793	0.0019	0.9478	492	11
GE30-10	0.65	101	0.1694	0.0019	9.9006	0.2510	0.4239	0.0102	0.9464	2278	46
GE30-13	0.14	357	0.0569	0.0007	0.5961	0.0155	0.0760	0.0018	0.9192	472	11
GE30-14	0.31	388	0.0615	0.0007	0.7625	0.0202	0.0899	0.0022	0.9203	555	13
GE30-15	0.07	628	0.0551	0.0007	0.4887	0.0143	0.0644	0.0015	0.7877	402	9
GE30-16	0.37	143	0.0646	0.0008	1.1238	0.0304	0.1263	0.0030	0.8908	767	17
GE30-17	0.21	530	0.0570	0.0007	0.5665	0.0153	0.0722	0.0018	0.9008	449	11
GE30-18	0.37	531	0.0555	0.0006	0.5463	0.0143	0.0714	0.0017	0.9172	445	10
GE30-19	0.15	463	0.0595	0.0007	0.7526	0.0196	0.0918	0.0022	0.9186	566	13
GE30-20	0.24	310	0.0671	0.0008	1.0986	0.0289	0.1188	0.0029	0.9154	724	16
GE30-21	0.13	269	0.0557	0.0013	0.5868	0.0231	0.0764	0.0018	0.5917	474	11
GE30-22	0.45	157	0.0614	0.0008	0.8462	0.0242	0.1000	0.0024	0.8539	614	14
GE30-23	0.19	379	0.0600	0.0007	0.6113	0.0160	0.0739	0.0018	0.9322	459	11
GE30-24	0.20	522	0.0558	0.0006	0.5632	0.0146	0.0732	0.0018	0.9387	455	11
GE30-25	0.33	619	0.0610	0.0007	0.7502	0.0191	0.0893	0.0022	0.9529	551	13
GE30-26	0.17	207	0.0587	0.0007	0.6752	0.0187	0.0834	0.0021	0.8945	516	12
GE30-27	0.55	1115	0.0593	0.0007	0.6642	0.0169	0.0813	0.0020	0.9569	504	12
GE30-28	0.07	386	0.0590	0.0008	0.6840	0.0196	0.0842	0.0020	0.8098	521	12
GE30-30	0.13	790	0.0564	0.0007	0.5204	0.0137	0.0670	0.0016	0.9335	418	10
GE30-31	0.70	738	0.0550	0.0006	0.4494	0.0119	0.0593	0.0015	0.9206	371	9
GE30-32	0.11	689	0.0544	0.0010	0.4753	0.0174	0.0634	0.0015	0.6646	396	9
GE30-33	0.69	222	0.1939	0.0022	13.6663	0.3535	0.5112	0.0125	0.9422	2662	53
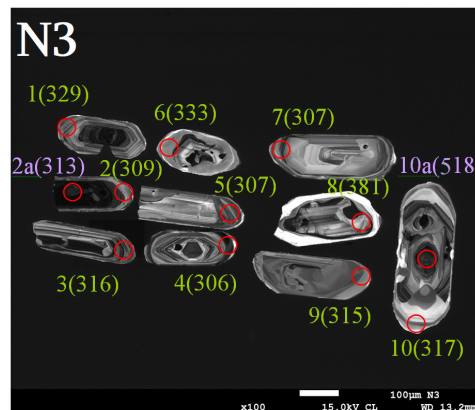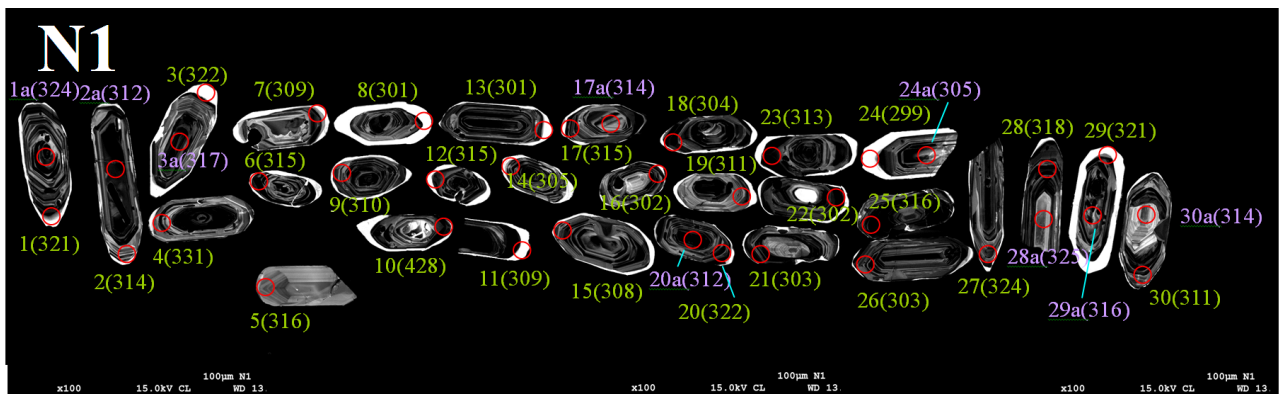
Fig. S1. Cathodoluminescence images of dated zircons from the pre-Alpine crystalline basement of the Pass sub-zone, Greater Caucasus. Circles define position of laser spots and are labeled with analysis number, values in parantheses are $^{206}Pb/^{238}U$ age and 1 uncertainty (in Ma). Analyses from grain cores are in purple.
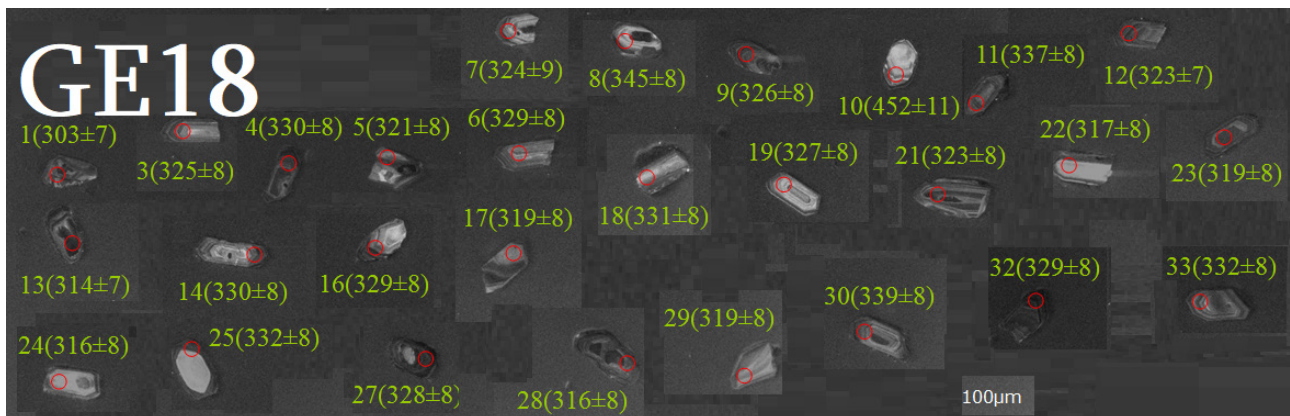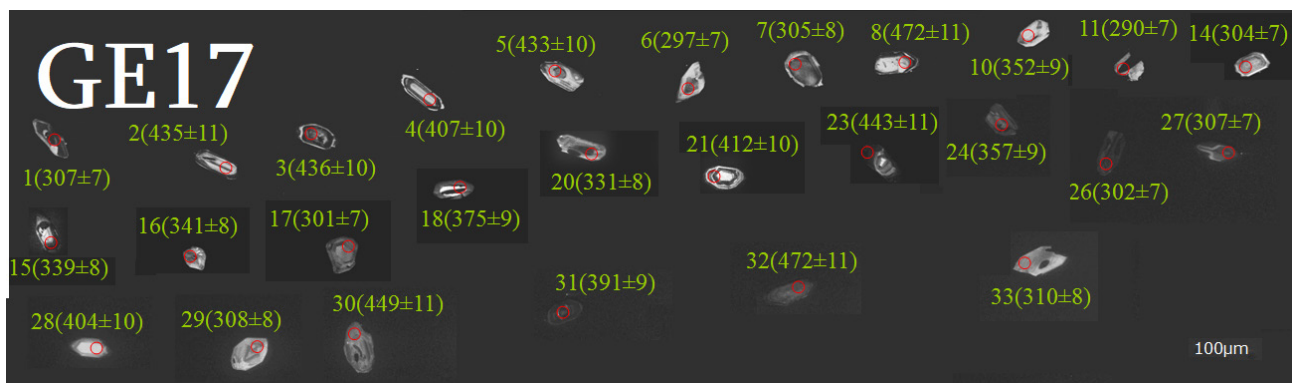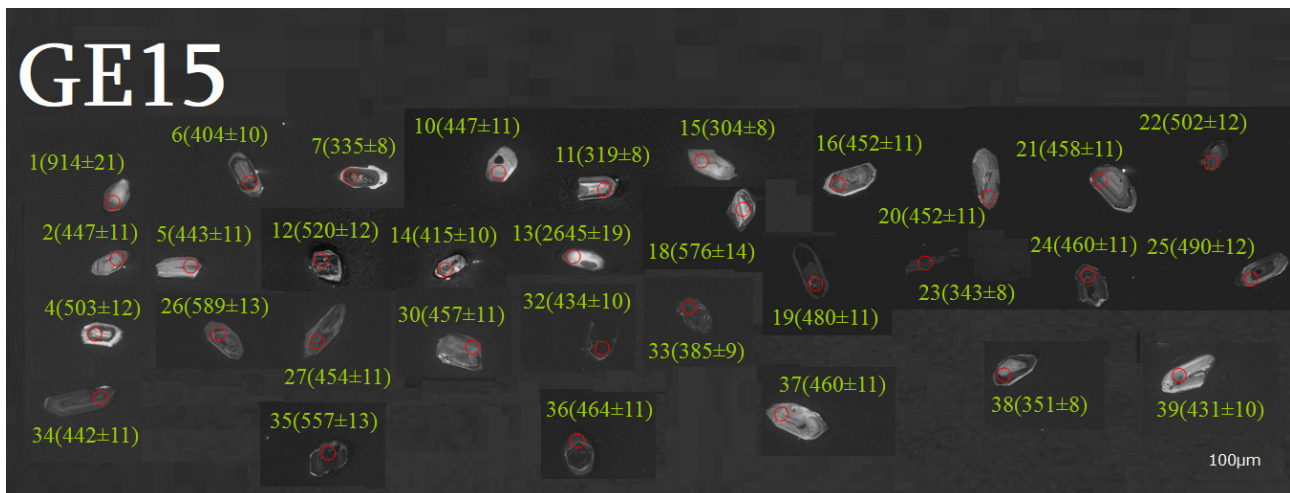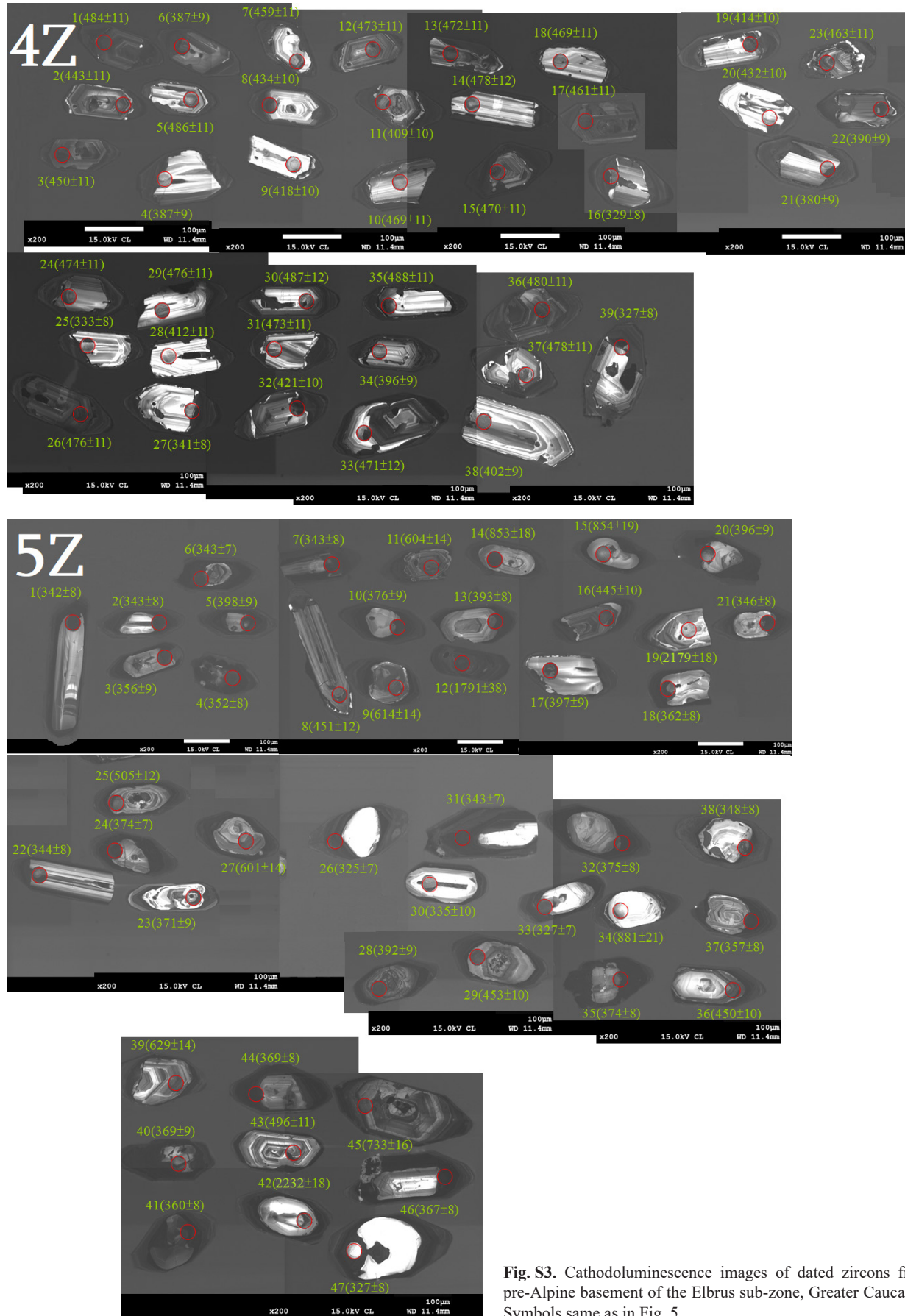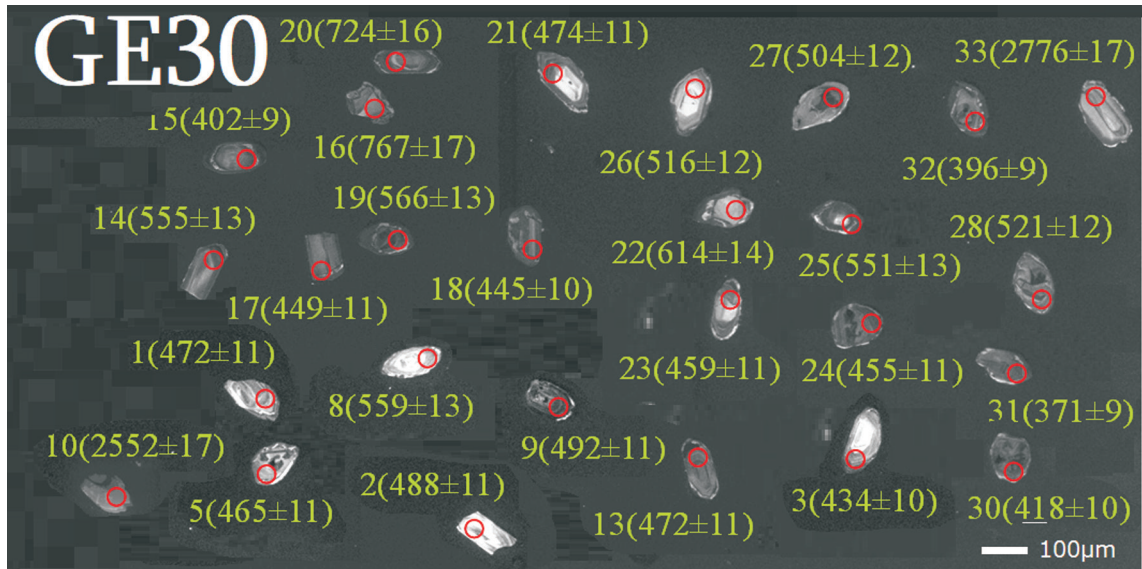
Fig. S1 (continued). Cathodoluminescence images of dated zircons from the pre-Alpine crystalline basement of the Pass sub-zone, Greater Caucasus. Circles define position of laser spots and are labeled with analysis number, values in parantheses are ^{206}Pb/^{238}U age and 1 uncertainty (in Ma). Analyses from grain cores are in purple.
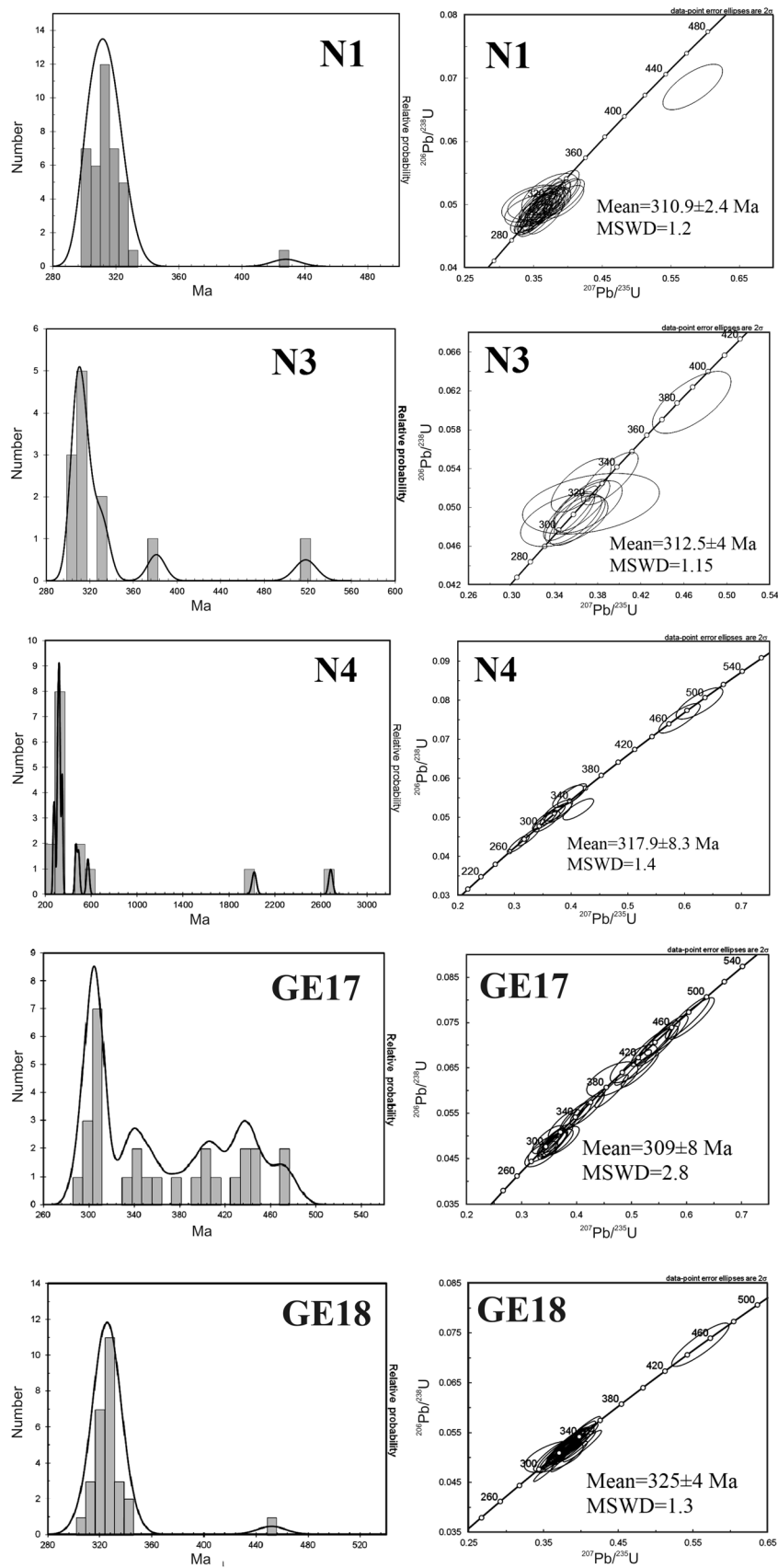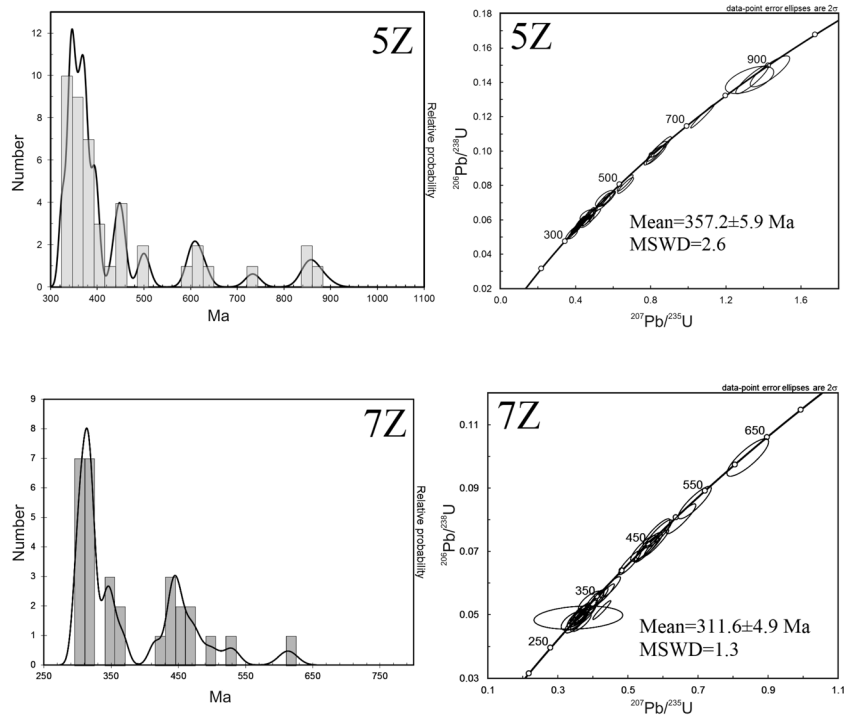
Fig. S2. Probability density curves for the analyzed zircons and Concordia diagrams for samples from the Pass sub-zone of the Greater Caucasus.

Fig. S3. Cathodoluminescence images of dated zircons from pre-Alpine basement of the Elbrus sub-zone, Greater Caucasus. Symbols same as in Fig. 5.

Fig. S3 (continued). Cathodoluminescence images of dated zircons from pre-Alpine basement of the Elbrus sub-zone, Greater Caucasus. Symbols same as in Fig. 5.

Fig. S4. Probability density curves for the analyzed zircons and Concordia diagrams for samples from the Elbrus subzone of the Greater Caucasus.